Forschungszentrum Karlsruhe
Technik und Umwelt

Wissenschaftliche Berichte
FZKA 6328
IAE-6137/3

Effect of Obstacle Geometry on Behaviour of Turbulent Flames

M. Kuznetsov, V. Alekseev, A. Bezmelnitsyn, W. Breitung, S. Dorofeev, I. Matsukov, A. Veser, Yu. Yankin

Institut für Kern- und Energietechnik
Projekt Nukleare Sicherheitsforschung

Juli 1999

Forschungszentrum Karlsruhe

Technik und Umwelt

Wissenschaftliche Berichte

FZKA 6328

IAE-6137/3

Effect of Obstacle Geometry on Behaviour of Turbulent Flames

M. Kuznetsov*, V. Alekseev*, A. Bezmelnitsyn*, W. Breitung,
S. Dorofeev*, I. Matsukov*, A. Veser, and Yu. Yankin*

Institut für Kern- und Energietechnik

Projekt Nukleare Sicherheitsforschung

* Russian Research Centre "Kurchatov Institute" Moscow, Russia

Forschungszentrum Karlsruhe GmbH, Karlsruhe
1999

Als Manuskript gedruckt

Forschungszentrum Karlsruhe GmbH
Postfach 3640, 76021 Karlsruhe

Mitglied der Hermann von Helmholtz-Gemeinschaft
Deutscher Forschungszentren (HGF)

ISSN 0947-8620

Zusammenfassung

Auswirkung der Hindernisgeometrie auf das Verhalten von turbulenten Flammen

Der Bericht beschreibt experimentelle Ergebnisse zur turbulenten Flammenausbreitung in teilweise versperrten Geometrien. Die Experimente wurden in einem 80 x 80 mm großen Rechteckkanal und in zylindrischen Rohren mit unterschiedlichen Innendurchmessern durchgeführt (174, 350, 520 mm). Der Versperrungsgrad betrug 9, 10, 30, 60 bzw. 90 % des gesamten Strömungsquerschnitts.

Die Verbrennungsabläufe wurden an Wasserstoff-Luft und stöchimetrischen H_2-O_2-Mischungen mit verschiedenen Zusätzen untersucht (N_2, Ar, He, CO_2). Alle Versuche wurden bei Umgebungstemperatur und -druck durchgeführt.

Die beobachteten Flammenausbreitungen lassen sich in vier charakteristische Regimes einteilen:

- Relativ langsame Flammen mit globalem Verlöschen der Verbrennung,
- Langsame instabile Verbrennungen mit mehreren separaten Flammenballen im Rohr,
- Beschleunigung von Flammen auf Überschallgeschwindigkeiten (choked flame), und
- Quasi-detonationen.

Für alle untersuchten Gemischklassen, Skalen und geometrische Konfigurationen trat das gesamte Spektrum von langsamen Flammen bis hin zu Quasidetonationen auf. Bei hinreichend großer Skala (Rohrlänge) hängt die Möglichkeit von schnellen Verbrennungsformen (choked flames, Quasi-detonationen) nur von der Gemischzusammensetzung ab. Für „starke" Mischungen bei denen Flammenbeschleunigung möglich ist, muß zusätzlich weitgehender geometrischer Einschluß und hinreichende Turbulenzerzeugung gegeben sein.

Zur Analyse der gemessenen Daten wurden verschiedene Mischungseigenschaften mit den beobachteten Flammenbeschleunigungen korreliert. Für die untersuchten Mischungen und thermodynamischen Anfangsbedingungen erwies sich das Expansionsverhältnis σ (= spezifisches Volumen des verbrannten Gases/spez. Volumen des unverbrannten Gases) als die beherrschende Größe. Schnelle Verbrennungsformen, wie „choked flame" und Quasidetonationen, sind nur möglich für Mischungen mit $\sigma > 3{,}75 \pm 0{,}25$. Dieser kritische Wert gilt für eine Anfangstemperatur von etwa 300 K, für magere und für reiche Wasserstoffgemische.

Die Auswirkungen der Mischungszusammensetzung und des Versperrungsgrades auf Deflagrations-Detonations-Übergang (DDT) wurden ebenfalls untersucht. Es zeigte sich, daß eine genügend kleine Detonationszellgröße, verglichen zum Rohrdurchmesser, ein notwendiges Kriterium für DDT darstellt. Allerdings unterscheiden sich Mischungen mit regulärer Detonationszellenstruktur (H_2-Ar, He) von solchen mit irregulärer Struktur (H_2-Dampf).

Abstract

EFFECT OF OBSTACLE GEOMETRY ON BEHAVIOR OF TURBULENT FLAMES

Results of experimental studies of turbulent flame propagation in obstructed tubes (channels) with different blockage ratios are presented. Explosion channel 80x80 mm and cylindrical tubes 174, 350, 520 mm i. d. were used in the tests. Blockage ratios were 0.09, 0.1, 0.3, 0.6, and 0.9. Explosion processes were studied in hydrogen-air and stoichiometric hydrogen-oxygen mixtures diluted with N_2, Ar, He, and CO_2. All tests were made with normal initial temperature and pressure.

Flame propagation in explosion channels resulted in one of four characteristic combustion regimes: relatively slow flames with global quenching, slow/unstable flames, choked flames, and quasi-detonations. The difference between slow regimes and fast regimes (choked flames and detonations) is shown to be the most pronounced for all mixtures, scales and geometrical configurations tested. At sufficiently large scale, possibility of development of fast combustion regimes is shown to depend only on mixture composition. Mixture properties, thus, are shown to provide a *potential* for effective flame acceleration. This potential can be realized, if geometry of confinement and scale provide favorable conditions for flame acceleration. Correlations of potential for flame acceleration with mixture properties are discussed. For mixtures and initial thermodynamic conditions used in the tests, mixture expansion ratio is shown to be the most significant parameter in these correlations. Fast combustion regimes are found to be only possible in mixtures with $\sigma > \sigma^* = 3.75 \pm 0.25$. This critical value can be a function of mixture type and initial conditions.

Effects of mixture composition and blockage ratio on DDT conditions are also discussed. The requirement of small enough mixture detonation cell size λ compared to characteristic size of a tube (channel) is confirmed as the necessary condition for onset of detonations. Critical conditions for onset of detonations in mixtures with regular cellular structure (Ar and He dilution) are shown to be different from those for irregular mixtures.

Inhaltsverzeichnis

Nomenclature

Latin

c_{sr} - sound speed in reactants;

c_{sp} - sound speed in combustion products;

D - tube diameter;

d - obstacle orifice diameter;

E_a - effective activation energy;

h - obstacle height;

L - obstacle spacing;

L_T - integral length scale of turbulence;

Le - Lewis number;

R - gas constant;

Re_T - turbulent Reynolds number;

S_L - laminar flame speed;

S_T - turbulent burning rate;

T_b - maximum flame temperature;

T_u - initial mixture temperature;

U - flow speed

u' - r.m.s. turbulent fluctuation velocity;

V - visible flame speed (laboratory frame);

V_{max} - maximum visible flame speed;

Greek

$\beta = E_a(T_b - T_u)/(RT_b^2)$ - Zeldovich number;

γ_r - ratio of specific heats in reactants;

$\delta = S_L\tau = \chi(T_b)/(S_L\sigma)$ - laminar flame thickness;

λ - detonation cell width;

ν - kinematic viscosity;

σ - ratio of densities of reactants and products (expansion ratio);

χ - thermal diffusivity;

1. Introduction.

The influence of mixture properties and scale on the regime of turbulent flame propagation in obstructed areas was studied in the previous work [1]. The following parameters were chosen to analyze effect of mixture properties on turbulent flame propagation in obstructed areas: L_T/δ, σ, S_L/c_{sr}, S_L/c_{sp}, and γ_r Le, β. where L_T, σ, S_L, δ, c_{sr}, c_{sp}, γ_r, Le, and β are integral length scale of turbulence, expansion ratio, laminar flame velocity, characteristic laminar flame thickness, sound speed in reactants, isobaric sound speed in combustion products ratio of specific heats in reactands, Lewis number, and Zeldovich number correspondingly. Lewis number is a ratio of thermal diffusivity to molecular diffusivity; Zeldovich number β is defined through effective activation energy of chemical reaction E_a and temperatures of unburned T_u and burned T_b mixture $\beta = E_a(T_b - T_u)/(RT_b^2)$.

Four character regimes of turbulent flame propagation in obstructed areas with BR = 0.6 were distinguished: (I) slow (subsonic) unstable flame propagation with global quenching; (II) slow unstable flames (subsonic regime with local quenching and following reignition); (III) regime of choked flame propagation with nearly-sonic velocity, and regime with development of choked flames with following transition to quasi-detonation.

All the tests in [1] were made with the same configuration of obstacles and blockage ratio BR = 0.6. This configuration was very favorable for effective flame acceleration. It is important to generalize the results for wider range of different geometrical conditions. Since the process of the flame acceleration depends significantly on the turbulence generation in the flow ahead the flame, obstacles play an important role in the process. A configuration of obstacles can be considered as a parameter which effects the flame acceleration.

Main objective of the present study is to obtain data on the effect of obstacle configuration, integral scale and mixture properties on behavior of the turbulent flames in obstructed areas.

2. Experimental details

Three tubes (174, 350, and 520 mm id) and explosion channel (80x80mm cross section) were used in the tests. Blockage ratios BR were 0.09, 0.1, 0.3, 0.6, and 0.9.

TORPEDO tube (520 mm id) was 33.5 m in length. It was equipped with annular obstacles. Blockage ratios BR were equal to 0.09, 0.3, and 0.6. Total number of obstacles was 65 with one-diameter distance between obstacles. Detailed description of the tube is given in [1].

FZK tube (350 mm id) was 12 m length. Only one configuration of obstacles with BR = 0.6 was used in this tube. Obstacles were spaced by a distance of one tube diameter.

DRIVER tube (174 mm id) was 11.5 m in length. Total number of obstacles was 65. They were spaced by one diameter. Tests with BR equal to 0.09, 0.3, and 0.6 were made. Detailed description of the tube is given in [1].

Square explosion channel (80x80mm cross section) was equipped with obstacles mounted onto the bottom and ceiling of the channel. Total number of obstacles was 65. They were spaced by one diameter. Blockage ratios were 0.1, 0.3, 0.6, and 0.9.

Pressure transducers, photodiodes and ion probes were used to record shock and flame dynamics. In addition, a total portion of burnt mixture was controlled by resulting pressure decrease after completing the combustion process and thermal equilibration.

Hydrogen-air mixtures (lean and rich) and stoichiometric hydrogen-oxygen mixtures diluted by inert gases (N_2, Ar, He, CO_2) were used in the tests. All tests were made with normal initial temperature and pressure. Thermodynamic characteristics of test mixtures were determined from [2, 3], cell size and laminar flame speed were approximated by [4-8].

3. Results

Experiments on turbulent flame propagation were performed with all tested mixtures mainly using DRIVER tube (174 mm id) and FZK tube (350 mm id). Some mixtures were tested at smaller scale (explosion channel) and at large scale using TORPEDO tube (520 mm id). Experimental conditions and resulting explosion modes are presented in Tables 1-4 for each of the facilities. Experiments are grouped by diluent gas and by blockage ratio.

The regimes of flame propagation are marked as follows in Tables 1-4. "Unstable/quench" - relatively slow flame propagation resulted in global extinguishing of flame at some distance along the tube. "Unstable/slow" - the same, but in the cases flame reached the end of the tube. "Choked flames" denotes development of sonic or choked flames. Term "quasi-detonation" corresponds to resulting initiation of detonations with velocity deficit (BR > 0.1). Term "detonation" - corresponds to initiation of detonation (BR = 0.09).

3.1. Characteristic regimes of turbulent flame propagation

Characteristic features of combustion regimes in obstructed tubes can be distinguished through analysis of X-t diagrams of flame propagation. Examples of such diagrams are presented in this section. The diagrams are plotted using data of pressure transducers, photodiodes and ion probes. Pressure transducers used in the tests are sensitive to heat flux from flames. Special measures to decrease or delay this effect were made, however this was relatively successful only for fast combustion regimes because of short times of processes. To avoid misinterpretation of pressure data in cases of slow flames, pressure curves are shown only for time intervals before flame arrival to the location of a transducer.

Unstable/quench. A characteristic X-t diagram of slow flame propagation with global extinguishing of the flame is shown in Fig. 1. Flame accelerates along first half of the tube reaching velocity of about 90 m/s. Data of photodiodes and ion probes located at the end of the tube do not show signals typical for flame arrival. This, of course, is not a sufficient indication of global extinguishing of the flame, since sensitivity of the transducers could principally be not high enough to resolve combustion process beyond 6.7 m in Fig. 1. However this kind of data in most cases were found to be consistent with total amount of fuel consumed in the process (see Tables 1 - 4). Such a consistency of

three types of measurements (photodiodes, ion probes, and global pressure change after thermal equilibration) was used to determine whether or not global extinguishing of combustion process was observed.

Unstable/slow. Examples of X-t diagrams for relatively slow flames are presented in Figs 2 - 11. Slowest flames were observed with BR = 0.1. Figures 2-4 show examples of such processes in explosion channel for hydrogen-lean mixture (Fig. 2), rich mixture (Fig. 3), and lean mixture in largest tube (Fig. 4). Initial flame acceleration is accompanied by pressure rise. Because flame propagation speeds are essentially subsonic, pressure waves are not formed and pressure transducers show global pressure increase and decrease in all the tube. The rate of initial pressure rise depends on competition between heat generation by combustion processes and heat losses. The maximum overpressures are well below the level defined by the adiabatic complete combustion overpressure for a given mixture. The overall pressure rise is followed by pressure decrease. This change has immediate effect on flame speeds (see Figs. 2 and 3). This is due to the fact that under conditions of the excess of heat losses over heat generation, expansion of combustion products does not occur, and visible flame speed should decrease. We need to notice that hydrogen combustion results in mole decrease in the reaction.

Combustion processes with BR = 0.3 are shown in Figs. 5 - 7. Flame speeds and maximum overpressures are higher in this case compared to BR = 0.1, even for less reactive mixtures. Other characteristic features of flame propagation (quasi-static pressure rise and effect of heat losses) are similar to those in Figs. 2 - 4.

Figures 8 and 9 show examples of X-t diagram of strongly unstable flame with local flame quenching and reignition observed in tests with BR = 0.6. The process shown in Figs. 8-9 generate a pressure wave, which propagates along all the tube ahead of the flame. The leading flame tongue propagates with a speed varying from 100 to 300 m/s. At certain conditions this tongue appears to be quenched, probably by a high level of turbulence. The quenching is followed by reignition downstream. Flame propagates locally both upstream and downstream after reignition. Figure 8 shows that several quenching-reignition cycles can occur during a single passage of a pressure wave to the end of the tube. Such a flame 'gallop' is not connected with large reverberations of pressure waves. Despite of high local speeds of flame propagation, the global propagation speed of the process is still well below sound speed in combustion products, which is typical for choked flames.

Choked flames. Figures 10 and 11 show examples of X-t diagrams of fast combustion regimes. Initial flame acceleration results in development of so-called 'choked' or 'sonic' flames. This combustion regime was studied in detail in [9-11]. The characteristic feature of this regime is quasi-steady speed of propagation, which is close to isobaric sound speed in combustion products.

Quasi-detonations. Example of X-t diagram of the fastest combustion regime observed is shown in Fig. 12. Fast flame acceleration results in formation of detonation wave at a distance close to 4 m in this particular case. The explosion wave propagates with nearly constant speed through all remaining part of the mixture. The speed of propagation is somewhat below the CJ speed. The velocity deficit is mainly due to momentum losses in the obstacle field. This deficit was found to increase with BR.

3.2. Effect of obstacle configuration

BR = 0.9. Limited number of tests were made with BR = 0.9. Results are presented in Figs. 13 and 14. Dependencies of flame propagation velocities on dimensionless distance (distance x over tube diameter D) along the tubes are shown. Fast combustion regimes are shown with black symbols, slow regimes with open symbols.

Slow combustion regimes were observed in most of tests. Flames did not reach the end of the tube in these tests. Complete quenching of flames was observed at about ¼ of the tube length.

Fast combustion regimes were observed for 13% of hydrogen in hydrogen-air mixture. Flame propagation at a quasi-steady speed was observed after initial acceleration phase. This speed was close to the sound speed in reactants.

BR = 0.6. Dependencies of flame propagation velocities on dimensionless distance (distance x over tube diameter D) along the tubes are presented in Figs. 15 - 24. Each of figures combine data from different tubes for the same type of mixtures. Fast combustion regimes (choked flames and quasi-detonations) are shown with black symbols, slow regimes with open symbols.

Figures 15 - 24 show that flame acceleration rate depends on scale. At the same time, the final regime (slow or fast) of flame propagation depends mainly on mixture composition. Most of the data show a significant difference in flame propagation speeds between slow and fast flames. Different characteristic speeds are observed also for fast flame and detonations in part of the figures.

BR = 0.3. Dependencies of flame propagation velocities on dimensionless distance (distance x over tube diameter D) along the tubes are presented in Figs. 25 - 30. Fast combustion regimes (choked flames and quasi-detonations) are shown with black symbols, slow regimes - with open symbols.

Slow combustion regimes were observed in tests with BR = 0.3 for the same range of mixtures as that with BR = 0.6. As different from results with BR=0.6, choked flames were observed within a narrower range of concentrations compared to that with BR=0.6. For example, for N_2 -diluted mixtures they were in the range of 12-13% H_2. Combustion of 9% H_2 mixture (He-diluted) resulted in either global quenching, or quasi-detonation process. This is due to the fact that the critical cell sizes for DDT are smaller in the case of BR = 0.3 compared to that with BR = 0.6 in the same tube [12].

It should be noted that the difference between fast flames and detonations was less pronounced with BR = 0.3, compared to that with BR = 0.6. Sometimes, it was even difficult to decide whether a combustion process resulted in DDT or not (see, e. g., Fig. 25). The difference between slow and fast combustion regimes was, however, clear in most of cases.

BR = 0.09 - 0.1. Dependencies of flame propagation velocities on dimensionless distance (distance x over tube diameter D) along the tubes are presented in Figs. 31 - 38. Processes of flame propagation observed with blockage ratio BR $\approx$ 0.1 were different from that with larger BR. Effectiveness of the flame acceleration was significantly reduced in the tests with BR $\approx$ 0.1 compared to that with BR > 0.1. Such a small blockage didn't provide conditions for effective generation of turbulence in the flow ahead of the flame.

Global flame quenching was not observed in tests with BR ≈ 0.1. In all the tests flame reached the end of the tubes. However, completeness of combustion was not always 100%.

Choked flames were not formed in the tests with BR ≈ 0.1. In cases flames accelerated to speeds exceeding typical values for slow combustion regimes, transition to detonation was observed. This shows that for mixtures which were strong enough to support flame acceleration in tubes with BR ≈ 0.1, necessary DDT conditions were easily satisfied.

4. Discussion

4.1. Critical conditions for flame acceleration

A significant difference in flame propagation speeds between slow and fast combustion regimes gives a convenient and well-defined measure of effectiveness of flame acceleration. In the present discussion, critical conditions for flame acceleration are linked to ability of flames to accelerate resulting in choked flames or detonations. Results of the tests suggest that mixture properties are defining a potential for effective flame acceleration. This potential can be realized, if geometry of confinement (including scale) provides favorable conditions for effective flame acceleration.

To compare the critical conditions for different BR and scale, a definition of integral length scale of turbulence is required. Geometry of explosion channels used in the tests provide the following characteristic sizes: tube diameter D (channel height), obstacle spacing L (= D), height of an obstacle *h*, and obstacle orifice diameter *d*. This set of parameters defines, generally, the integral length scale of turbulence L_T. Shadow photographs of combustion processes in the explosion channel 80x80 mm [13] have shown that integral length scale (large eddy size) of turbulence is controlled by *h* for BR = 0.1 and by *d* for BR = 0.9. With BR = 0.3 and BR = 0.6, the size of the largest eddies appeared to be controlled by tube diameter and obstacle spacing. In accordance to these observations, the following definition of L_T was adopted:

$$\begin{aligned} L_T &= h = D\cdot(1-(1-BR)^{1/2})/2, && \text{for } BR \le 0.1; \\ L_T &= D = L, && \text{for } BR = 0.3 \text{ and } BR = 0.6; \\ L_T &= d = D\cdot(1-BR)^{1/2}, && \text{for } BR \ge 0.9. \end{aligned} \qquad (1)$$

Resulting combustion regimes are shown in Fig. 39 in variables of σ and L_T/δ. It is seen that for scale ratio $L_T/\delta < 100$, much more energetic mixtures (large σ) are required for effective flame acceleration compared to cases of $L_T/\delta > 100$. At sufficiently large scale ($L_T/\delta > 100$), the border between fast and slow combustion regimes is defined, mainly, by the value of mixture expansion ratio σ. The critical value of σ appeared to be $\sigma^* = 3.75 \pm 0.25$. Each type of mixtures gives a well defined critical σ-value. This critical value does not depend on scale (for $L_T/\delta > 100$) and on BR. Values of σ^*, however, are slightly different for different types of mixtures. They vary within a rather narrow range from 3.5 to 4.0 for the mixtures used in the tests.

Figure 40 shows effect of Lewis number on resulting combustion regime. Data with $L_T/\delta > 100$ are collected in Fig. 40. Lean and stoichiometric mixtures give critical values of σ very close to $\sigma^* = 3.75$. The differences in values of σ^* mentioned above are observed only for hydrogen-rich mixtures with Le > 1.

We need to notice, that mixtures and initial conditions used in the tests presented here do not permit an estimation of the effect of Zeldovich number β on critical conditions for effective flame acceleration. The combined effect of Le and β, which is important for behavior of laminar flames, cannot be addressed, as well, with the current set of data.

4.2. Critical conditions for DDT.

Critical conditions for DDT in tubes with different BR were analyzed in [12]. It was shown that a characteristic size D* of obstructed tube may be defined which correlates with detonation cell size λ of the critical mixture composition for DDT. The size D* is defined by the tube diameter D, BR and obstacle spacing L:

$$D^* = (L + D)/2/(1-d/D). \quad (2)$$

For L = D, what was the case in our tests:

$$D^* = D/(1-d/D), \text{ for } BR \geq 0.1. \quad (3)$$

For mixtures of hydrogen and hydrocarbon fuels with air, which are characterized by irregular cellular structures, the critical conditions for DDT was shown to agree with:

$$D^*/\lambda > 7, \quad (4)$$

within limits of accuracy of the cell size data.

Results for mixtures diluted with Ar and He, which are characterized by regular cellular structures, show that critical conditions for DDT expressed by Eqs. 3 and 4 are not valid for this types of mixtures. Figure 41 shows that a borderline between cases of DDT and deflagrations can be approximately described by:

$$D^*/\lambda > 40. \quad (5)$$

The difference in critical conditions for DDT between 'regular' and 'irregular' systems show the same trend as that in critical conditions for detonation propagation from a tube to an unconfined space. The critical exit diameter, expressed in terms of λ, has been found to be larger in regular systems compared with irregular ones.

Critical conditions for DDT expressed in terms of Eqs. 3, 4 and 5 show, that onset of detonation is facilitated with decrease of BR for the same tube diameter. This means that mixture compositions can be found, which are able to undergo DDT with, e. g., BR = 0.3, but are not with BR = 0.6. This is in accord with observations in the present tests.

A requirement of development of fast combustion regime prior to DDT can be considered as one of the necessary DDT conditions. An interplay of critical conditions for flame acceleration and for onset of detonation (Eqs. 4 and 5) define the range of compositions resulting in choked flames. In accordance with that, choked flames were observed for many mixtures with BR = 0.6; there were fewer cases of choked flames with BR = 0.3; there was no one case of a choked flame with BR = 0.1.

4.3. Effect of scale on propagation speed of slow flames.

While propagation speeds of fast combustion regimes (choked flames and detonations) depend mainly on thermodynamic properties of the mixture, propagation speeds of relatively slow flames depend on scale. Results of our previous study [1] showed this

effect qualitatively. Results of present tests with different blockage ratio can be used to highlight this effect.

Maximum visible flame speeds V_{max} for slow combustion regimes normalized with σS_L (speed of laminar flames relative to fixed observer) are plotted against L_T/δ in Fig. 42. Propagation speeds of relatively slow flames increase significantly with scale. Up to $L_T/\delta \approx 100$, $V_{max}/\sigma/S_L$ increases more or less linear with L_T/δ. Beyond this value, a kind of saturation is seen. This may be connected with well known change of characteristic regime of turbulent flame propagation with increase of level of turbulence. Turbulent Reynolds number Re_T can be expressed as:

$$Re_T = u' \cdot L_T/\nu \approx (u'/S_L) \cdot (L_T/\delta), \qquad (6)$$

where u' is r.m.s. turbulent fluctuations velocity, ν - viscose diffusivity. Equation 6 shows linear increase of Re_T with L_T/δ. In the range of relatively small Reynolds numbers, turbulent burning rate increases due to flame wrinkling. With further increase of turbulence level (Re_T) flame stretch should play a role, which tends to decrease the turbulent burning rate.

Figure 42 gives just a qualitative indication of increase of slow flame speeds with scale. Quantitative predictions of flame speeds is difficult to make using data of Fig. 42, not only because of a considerable scatter of data points, but also because speeds of flame propagation depends on actual geometrical configuration. Additional analysis is required in order to separate effect of mixture properties (such as Le, β, and σ) and geometrical configuration on the observed flame speeds.

5. Summary and conclusions

Processes of turbulent flame propagation in obstructed tubes (channels) with different blockage ratios have been studied. Explosion channel 80x80 mm and cylindrical tubes 174, 350, 520 mm i. d. were used in the tests. Blockage ratios were 0.09, 0.1, 0.3, 0.6, and 0.9. Explosion processes were studied in hydrogen-air and stoichiometric hydrogen-oxygen mixtures diluted with N_2, Ar, He, and CO_2. All tests were made with normal initial temperature and pressure.

Flame propagation in explosion channels has been found to result in one of the following four characteristic combustion regimes. Unstable/quench - relatively slow flame propagation with variable speed resulted in global extinguishing of flame at some distance along the tube. Unstable/slow - relatively slow flame propagation with variable speed, but in the cases flame reached the end of the tube. Choked flames - quasi-steady flame propagation with a speed close to isobaric sound speed in combustion products. Quasi-detonation - quasi-steady propagation of explosion wave with a speed somewhat below the CJ detonation velocity due to momentum losses in obstacle field.

It has been found that there are some differences in characteristic features of the flame propagation in obstructed areas with different blockage ratio. Global quenching and choked flames were not observed in the tests with BR 0.09 and 0.1. Large BR (0.6 and 0.9) resulted in relatively more unstable slow regimes of propagation compared to BR < 0.6.

It has been shown that scale plays an important role influencing rate of flame acceleration and propagation speed of slow flames; both tend to increase with scale in most cases.

Possibility of development of fast combustion regimes has been also found to depend on scale. However, at sufficiently large scale ($L_T/\delta > 100$), such a possibility was found to depend only on mixture composition.

The difference between slow regimes (unstable/quench and unstable/slow) and fast regimes (choked flames and detonations) has been found to be the most pronounced for all mixtures, scales and geometrical configurations tested. This difference gives a well-defined measure of effectiveness of flame acceleration. Mixture properties have been shown to provide a *potential* for effective flame acceleration. This potential can be realized, if geometry of confinement and scale provide favorable conditions for flame acceleration.

It has been shown that for mixtures and initial thermodynamic conditions used in the tests, the *potential* for effective flame acceleration is defined mainly by the value of mixture expansion ratio σ. Development of fast combustion regimes has found to be only possible in mixtures with $\sigma > \sigma^* = 3.75 \pm 0.25$. This critical value can be a function of mixture type and initial conditions.

DDT has been found to be possible only if (1) flames are able to accelerate to fast combustion regimes, and (2) detonation onset conditions are satisfied. The requirement of small enough mixture detonation cell size λ compared to characteristic size of a tube (channel) D* has been confirmed as the necessary condition for onset of detonations. Definition of $D^* = D/(1\text{-}d/D)$ has been found to provide appropriate description of changes of the critical conditions with variations of BR.

Critical conditions for onset of detonations in mixtures with regular cellular structure (Ar and He dilution) have been found to be more severe ($D^*/\lambda > 40$) compared to those for irregular mixtures ($D^*/\lambda > 7$).

6. References

1. Dorofeev S.B, M.S. Kuznetsov, V.I. Alekseev, A.A. Efimenko, A.V. Bezmelnitsyn, Yu.G. Yankin, and W. Breitung. Effect of scale and mixture properties on behavior of turbulent flames in obstructed areas. Preprint IAE-6127/3, Moscow, 1999, Report FZKA-6268, Karlsruhe, 1999.
2. Reynolds W.C., The Element Potential Method for Chemical Equilibrium Analysis: Implementation in the Interactive Program STANJAN Version 3, Dept. of Mechanical Engineering, Stanford University, Palo Alto, California, January 1986.
3. Reid R.C., J.M. Prausnitz, T.K. Sherwood. The properties of gases and liquids, 3rd edition, McGraw-Hill Book Company, NY, London, Tokyo, 1976.
4. Koroll G.W., R.K. Kumar, and E.M. Bowles. Burning velocities of hydrogen-air mixtures. *Combust. Flame* 94: 330-340 (1993)
5. Koroll G.W. and S.R. Mulpuru. The effect of dilution with steam on the burning velocity and structure of premixed hydrogen flames. Twenty-First Symposium (International) on Combustion/The Combustion Institute, pp. 1811-1819 (1986)
6. Kumar R.K. Detonation cell widths in hydrogen-oxygen-diluent mixtures. *Combust. Flame*, 80(2):157-169 (1990).
7. Knystautas R., J.H. Lee, and C.M. Guirao. The critical tube diameter for detonation failure in hydrocarbon-air mixtures. *Combust. Flame*, 48(1):63-83 (1982).
8. Gavrikov A.I., A.A. Efimenko, and S.B. Dorofeev. Detonation cell size predictions from detailed chemical kinetic calculations. Preprint IAE-6091/3, Moscow, 1998.
9. Peraldi O., R. Knystautas, and J.H. Lee. Criteria for transition to detonation in tubes. Twenty-First Symposium (International) on Combustion/The Combustion Institute, pp. 1629-1637 (1986).
10. Chan C.K. and D.R. Greig. The structure of fast deflagrations and quasi-detonations. Twenty-Second Symposium (International) on Combustion/The Combustion Institute, pp. 1733-1739 (1988)
11. Lee J.H., R. Knystautas, and C.K. Chan. Turbulent flame propagation in obstacle-filled tubes. Twentieth Symposium (International) on Combustion/The Combustion Institute, pp. 1663-1672 (1984)
12. S. B. Dorofeev, V. P. Sidorov, M. S. Kuznetsov, I.D. Matsukov, and V.I. Alekseev. Effect of scale on the onset of detonations. Submitted to 17th ICDERS, July25-30, 1999, Heidelberg, Germany (1999).
13. Kuznetsov M.S., I.D. Matsukov, V.I. Alekseev, and S.B. Dorofeev. Photographic study of unstable turbulent flames in obstructed channels. Submitted to 17th ICDERS, July25-30, 1999, Heidelberg, Germany (1999).
14. Teodorczyk A., J.H. Lee, and R. Knystautas. Propagation mechanism of quasi-detonations. Twenty-Second Symposium (International) on Combustion/The Combustion Institute, pp. 1723-1731 (1988)
15. A. Teodorczyk, J. H. S. Lee, R. Knystautas, In: AIAA Progress in Astroanautics and Aeronautics, v. 133, pp 233-240, 1990

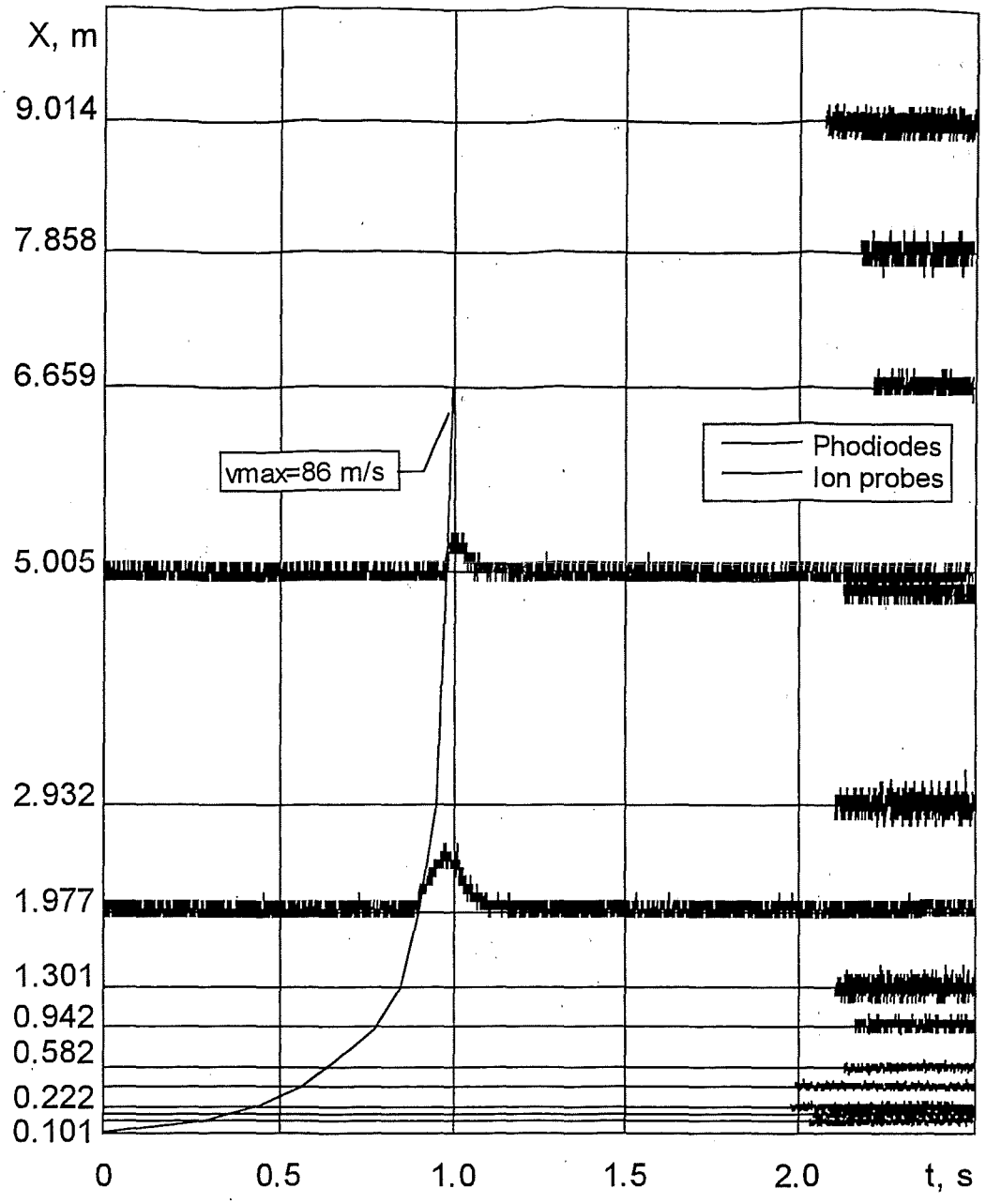

Figure 1: X-t diagram of flame propagation (slow/quench regime) in DRIVER tube (174 mm i. d.). Mixture: 11% $H_2/O_2/N_2$, BR = 0.3

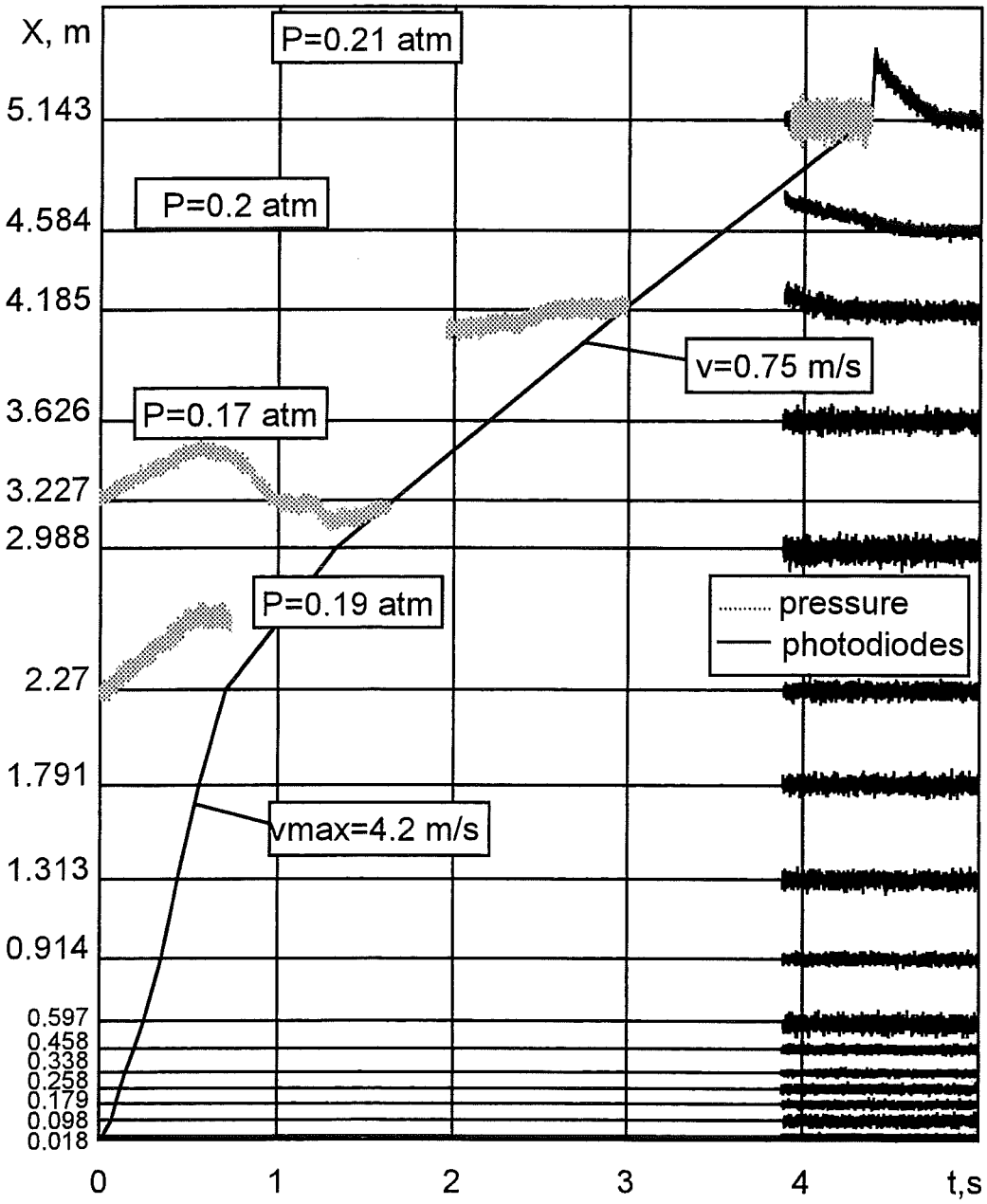

Figure 2: X-t diagram of flame propagation (slow/unstable regime) in channel 80x80 mm. Mixture: 11% H_2/air, BR = 0.1

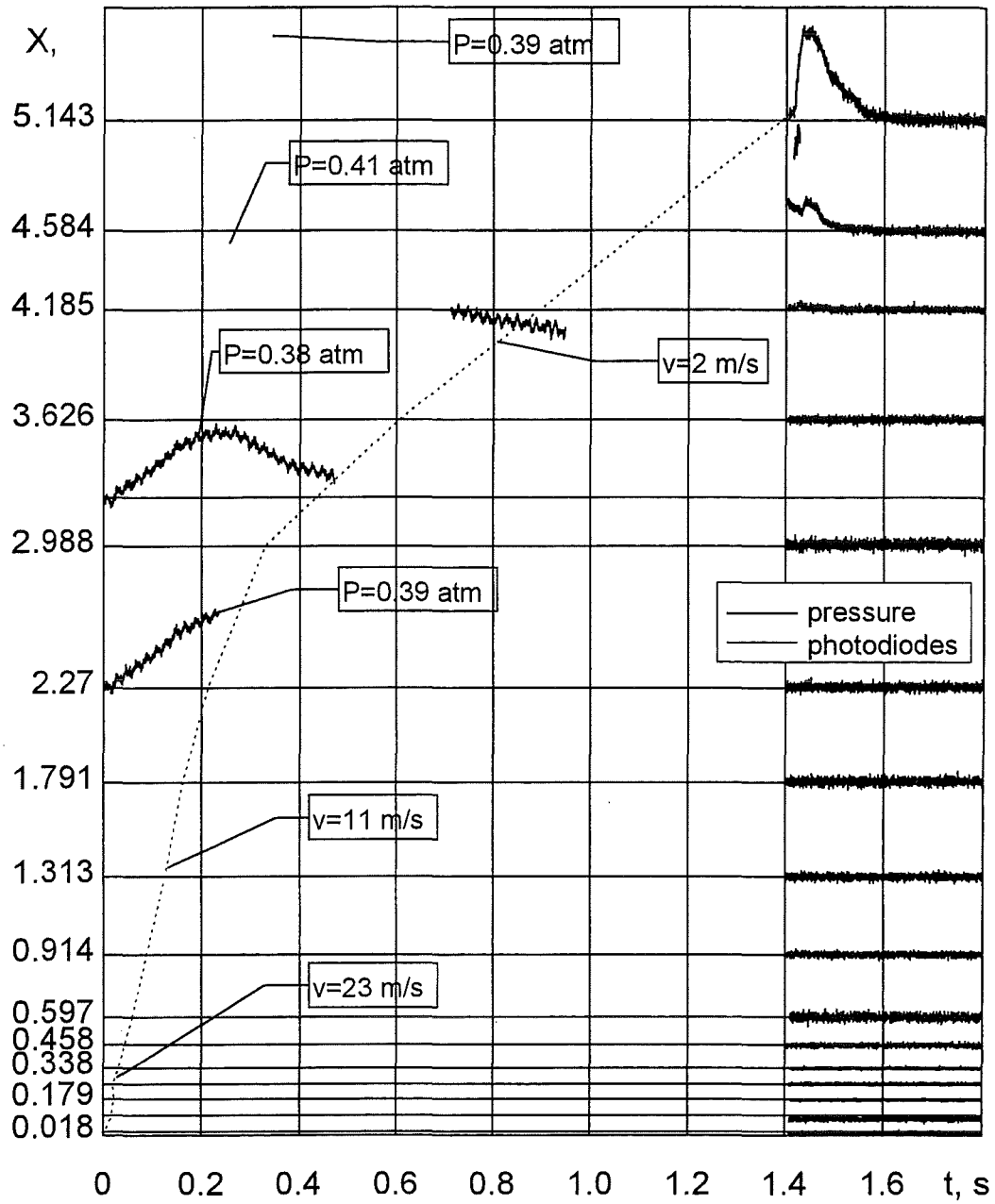

Figure 3: X-t diagram of flame propagation (slow/unstable regime) in channel 80x80 mm. Mixture: 70% H_2/air, BR = 0.1

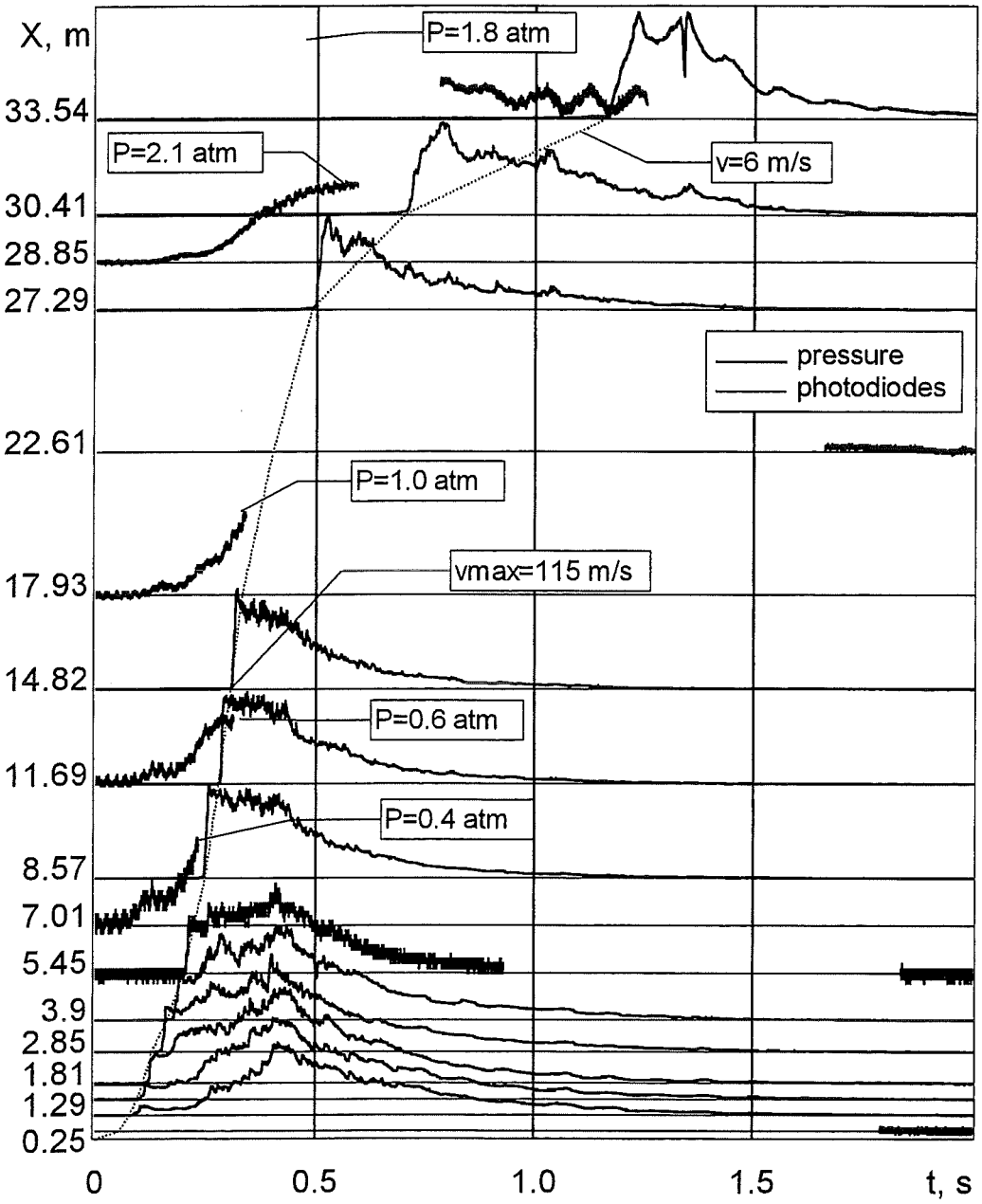

Figure 4: X-t diagram of flame propagation (slow/unstable regime) in TORPEDO tube (520 mm i. d.). Mixture: 16% H_2/air, BR = 0.1

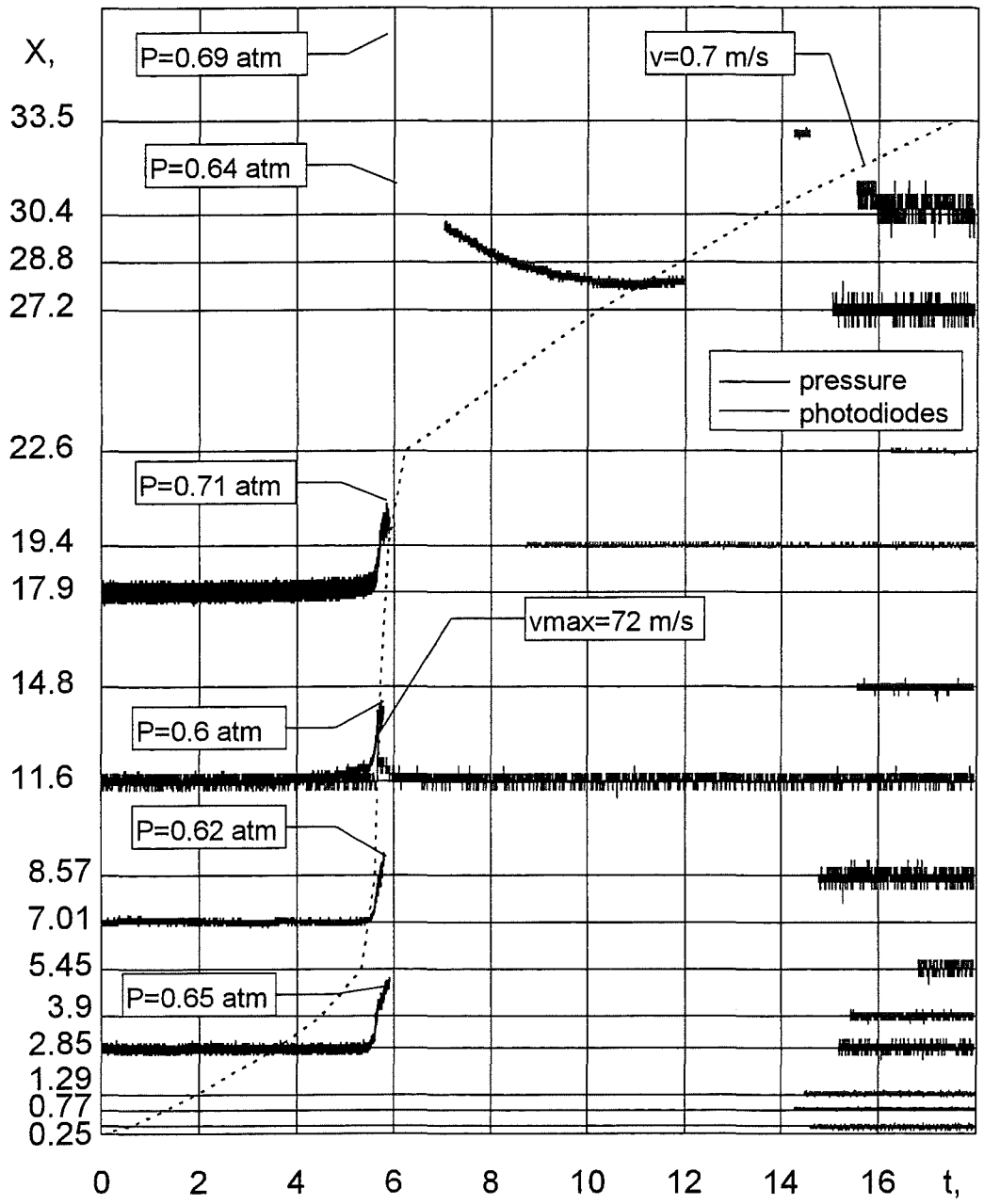

Figure 5: X-t diagram of flame propagation (slow/unstable regime) in TORPEDO tube (520 mm i. d.). Mixture: 9% H_2/air, BR = 0.3

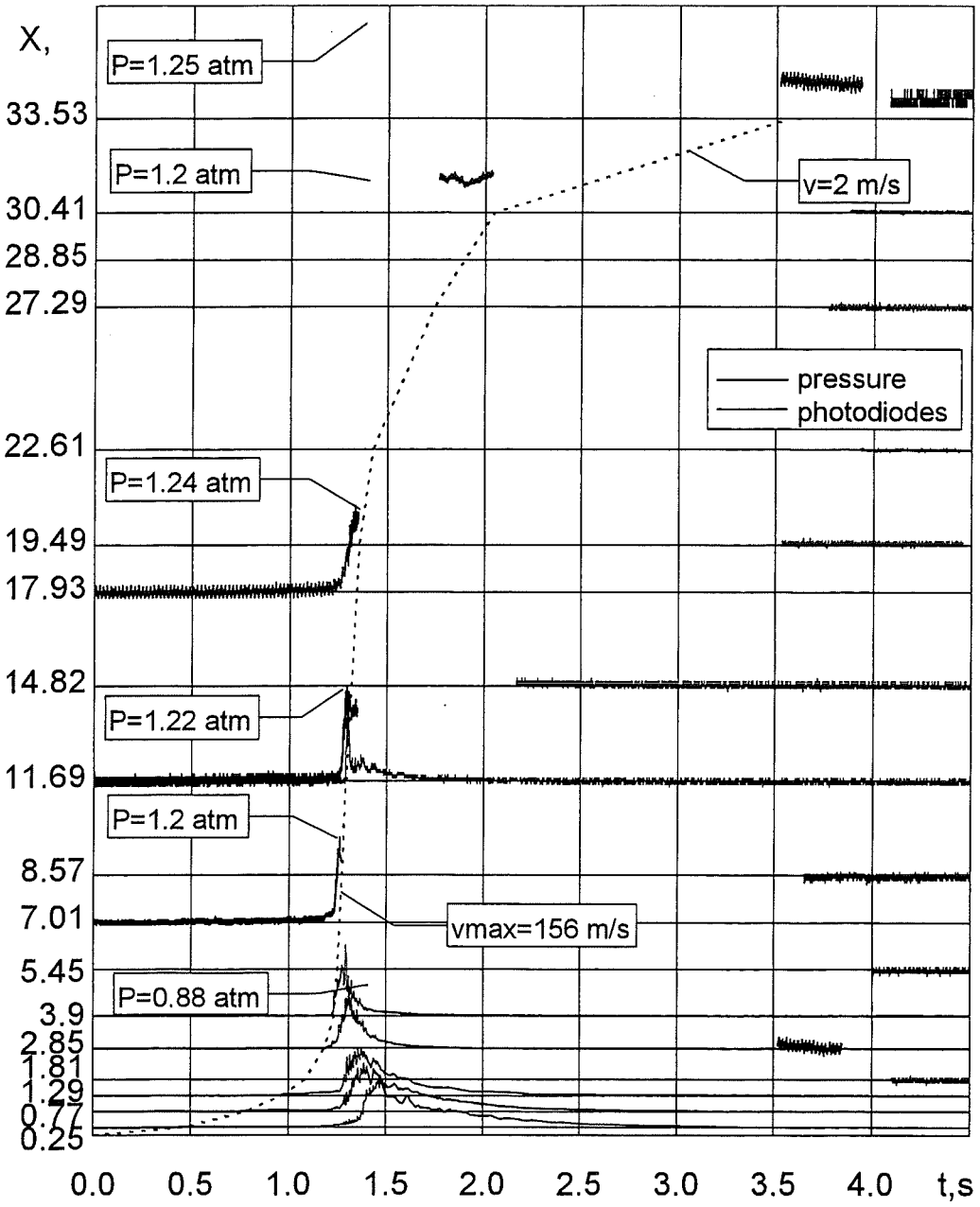

Figure 6. X-t diagram of flame propagation (slow/unstable regime) in TORPEDO tube (520 mm i. d.). Mixture: 10% H_2/air, BR = 0.3

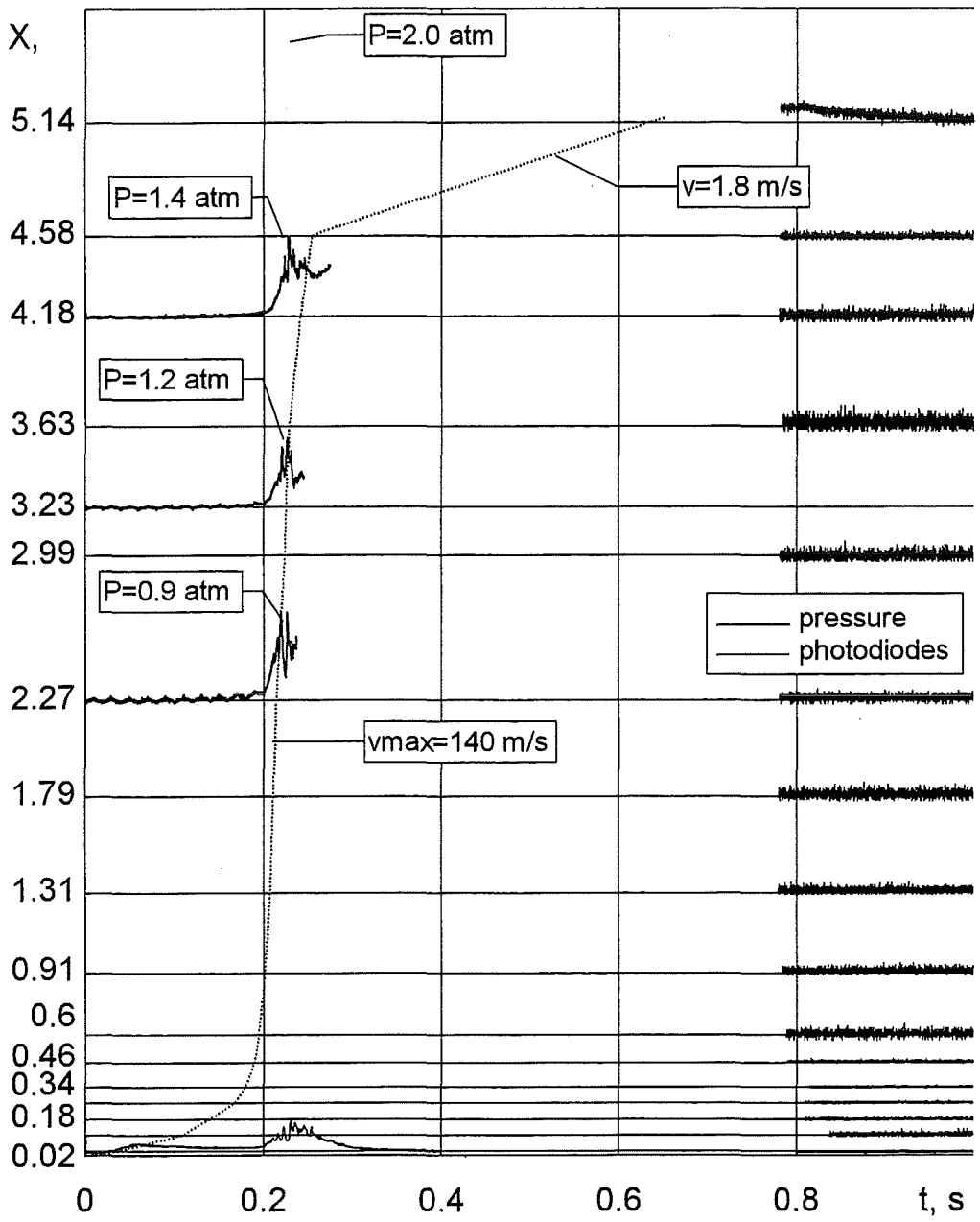

Figure 7: X-t diagram of flame propagation(slow/unstable regime) in channel 80x80 mm. Mixture: 10% H_2/air, BR = 0.3

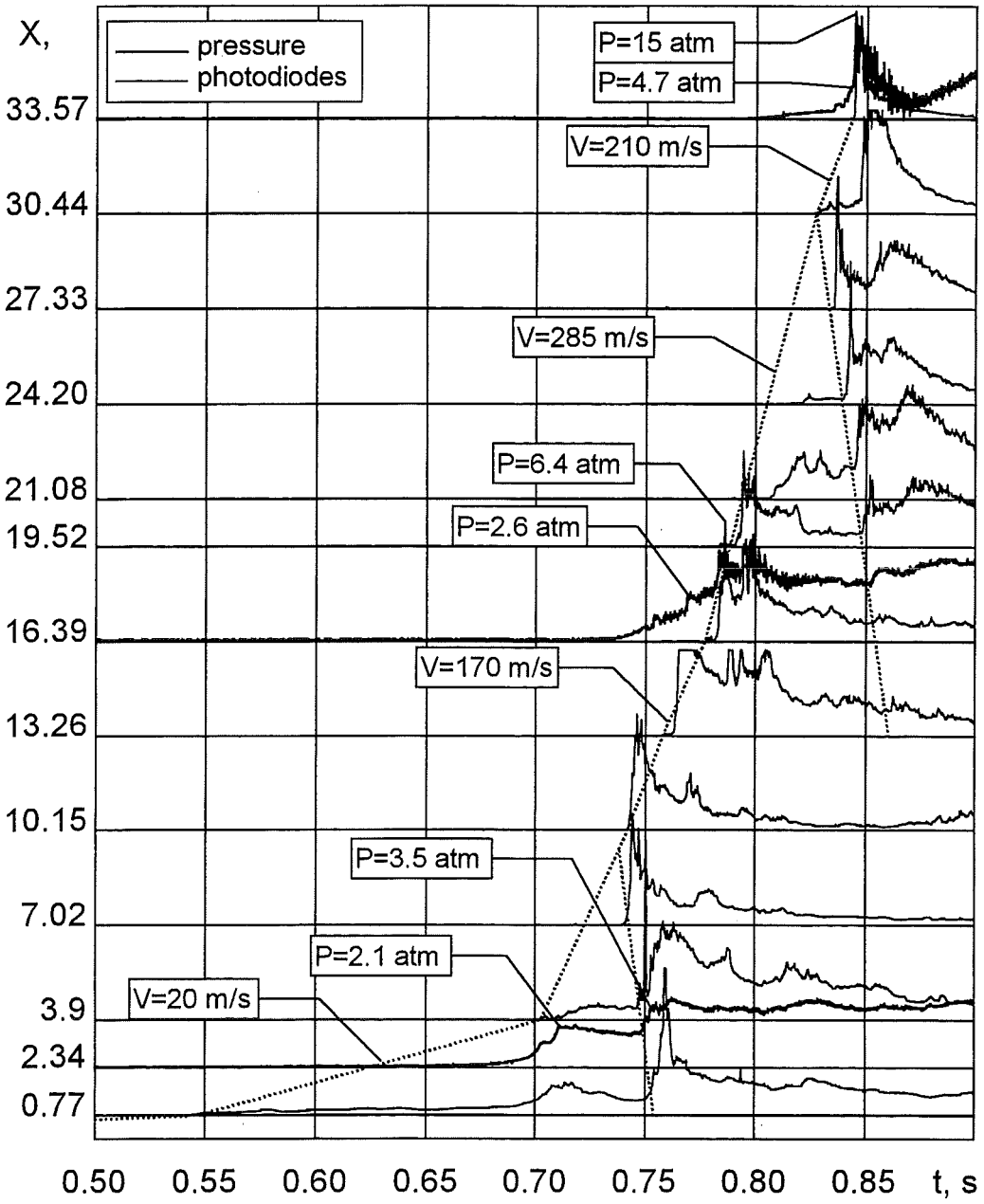

Figure 8: X-t diagram of flame propagation (slow/unstable regime) in TORPEDO tube (520 mm i. d.). Mixture: 9.5% H_2/air, BR = 0.6

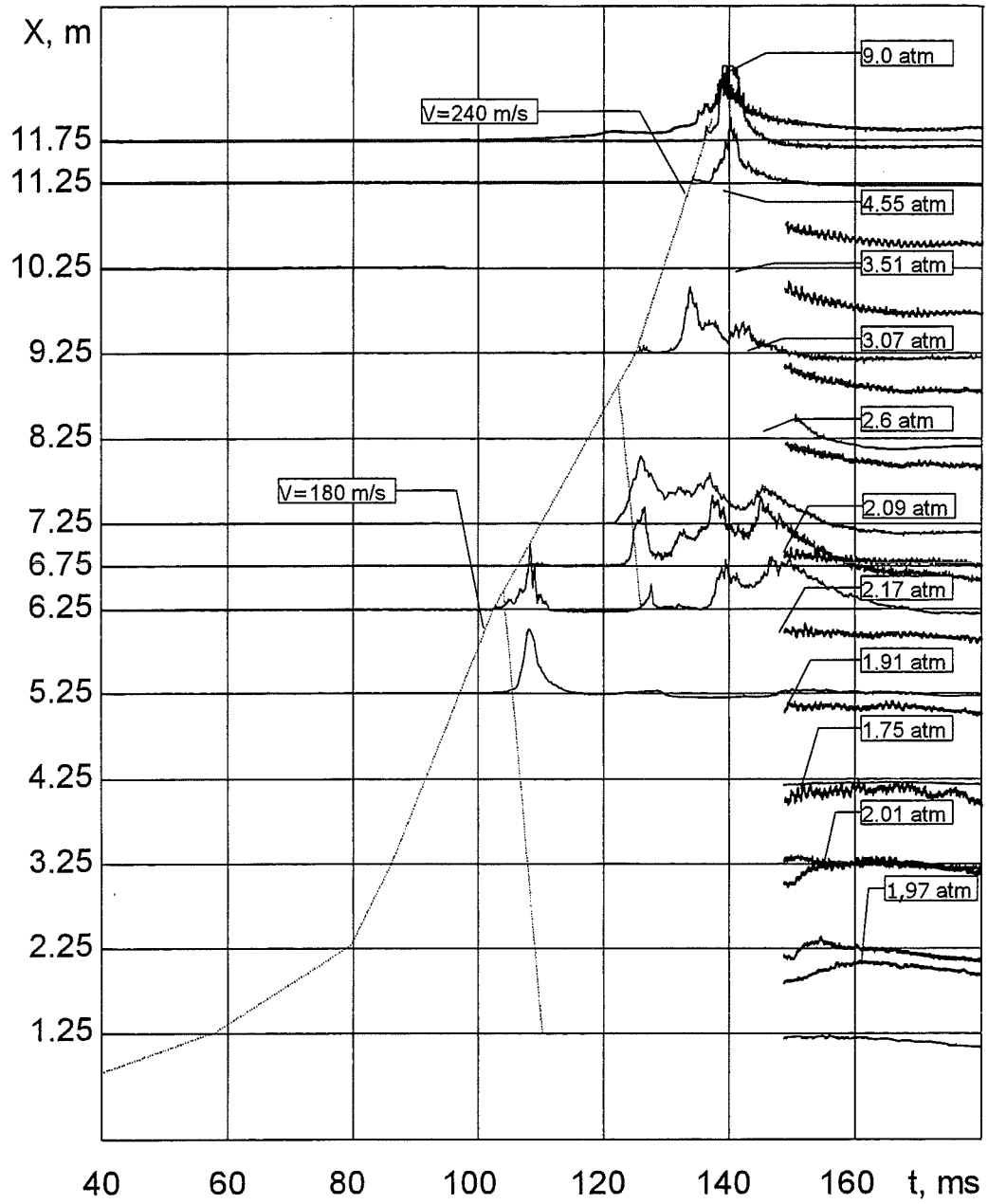

Figure 9: X-t diagram of flame propagation (slow/unstable regime) in FZK tube (350 mm i. d.). Mixture: 9% H_2/air, BR = 0.6

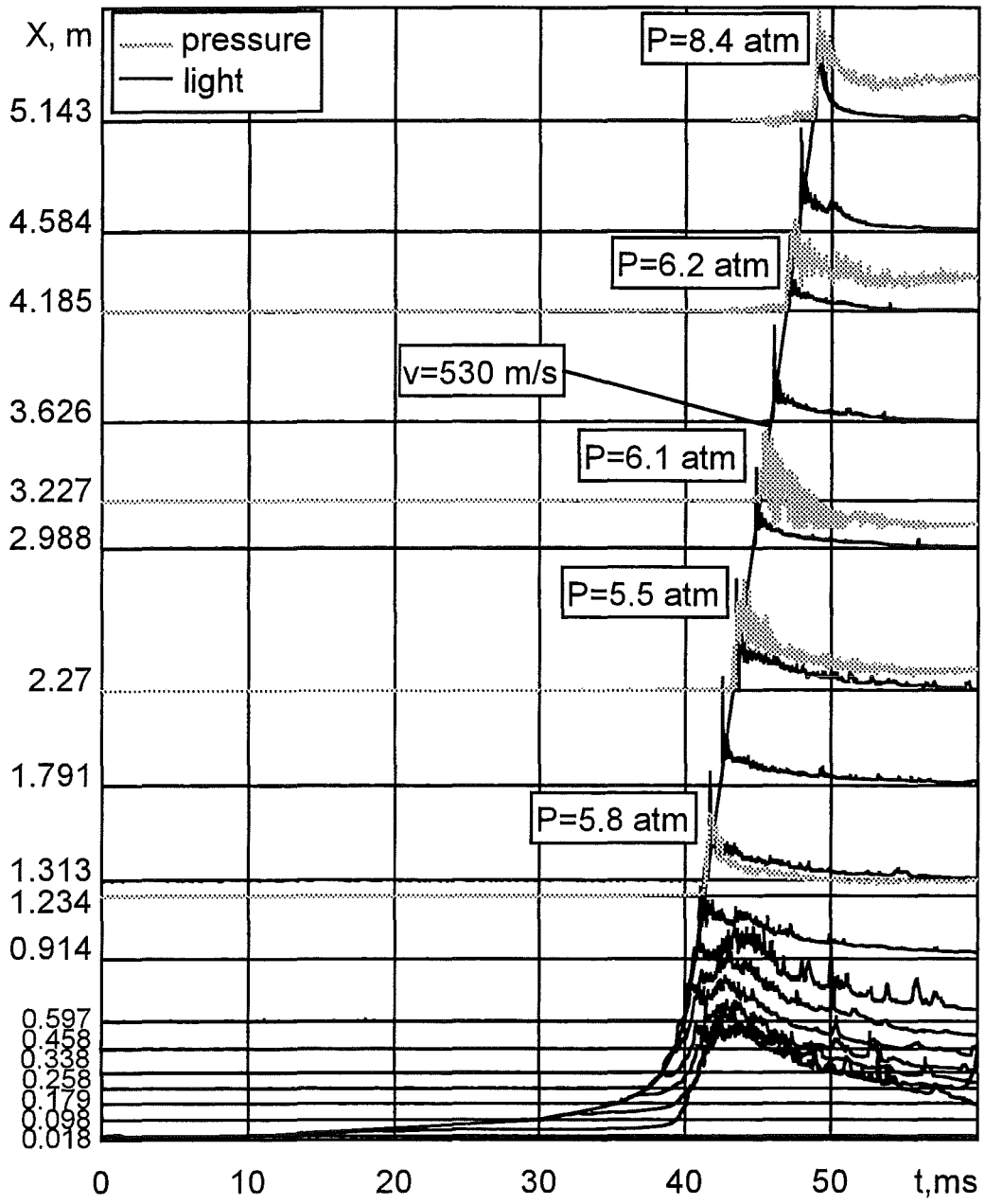

Figure 10: X-t diagram of flame propagation (sonic regime) in channel 80x80 mm. Mixture: 13% H_2/air, BR = 0.6

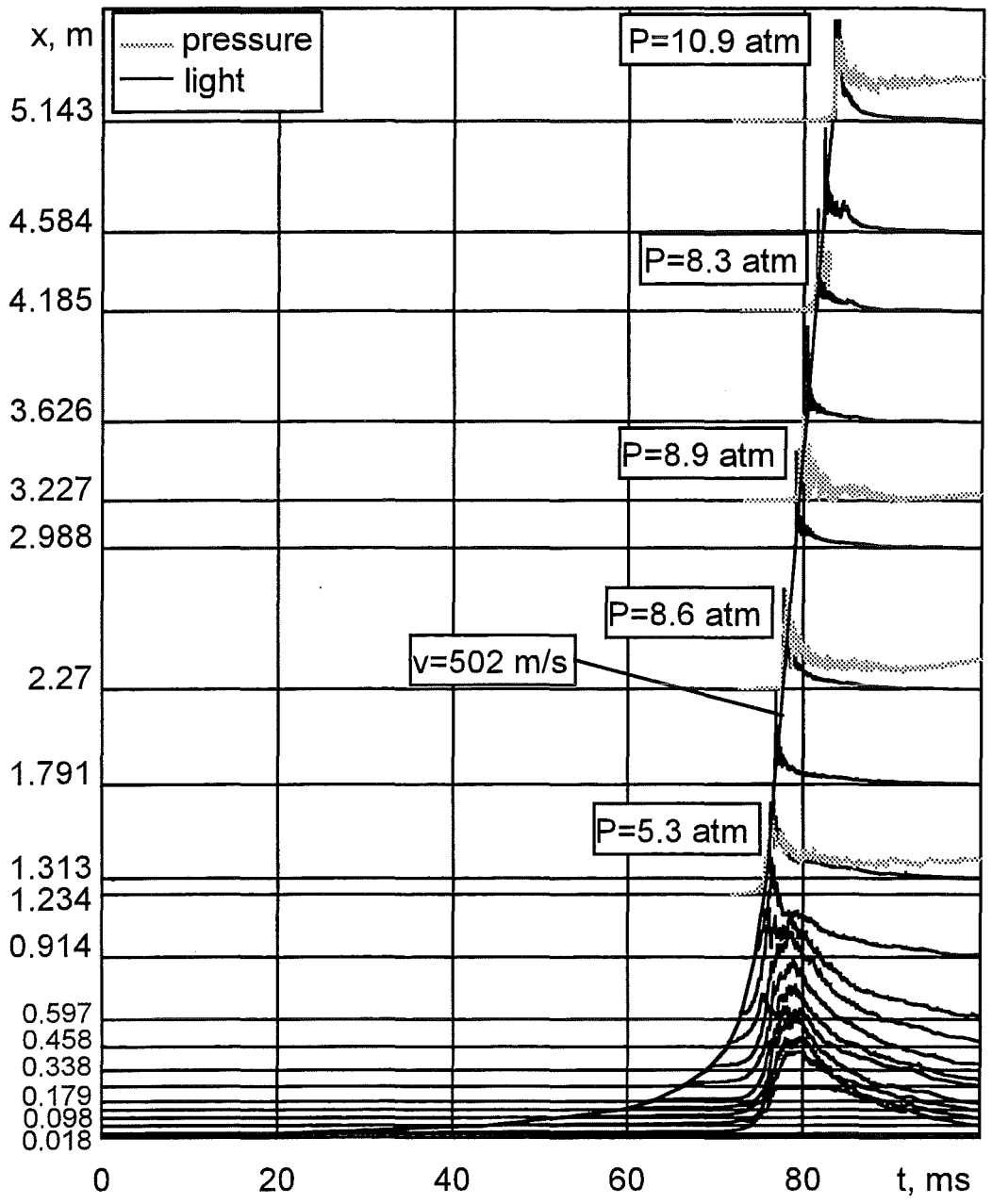

Figure 11: X-t diagram of flame propagation (sonic regime) in channel 80x80 mm. Mixture: 10% $H_2/O_2/Ar$, BR = 0.6

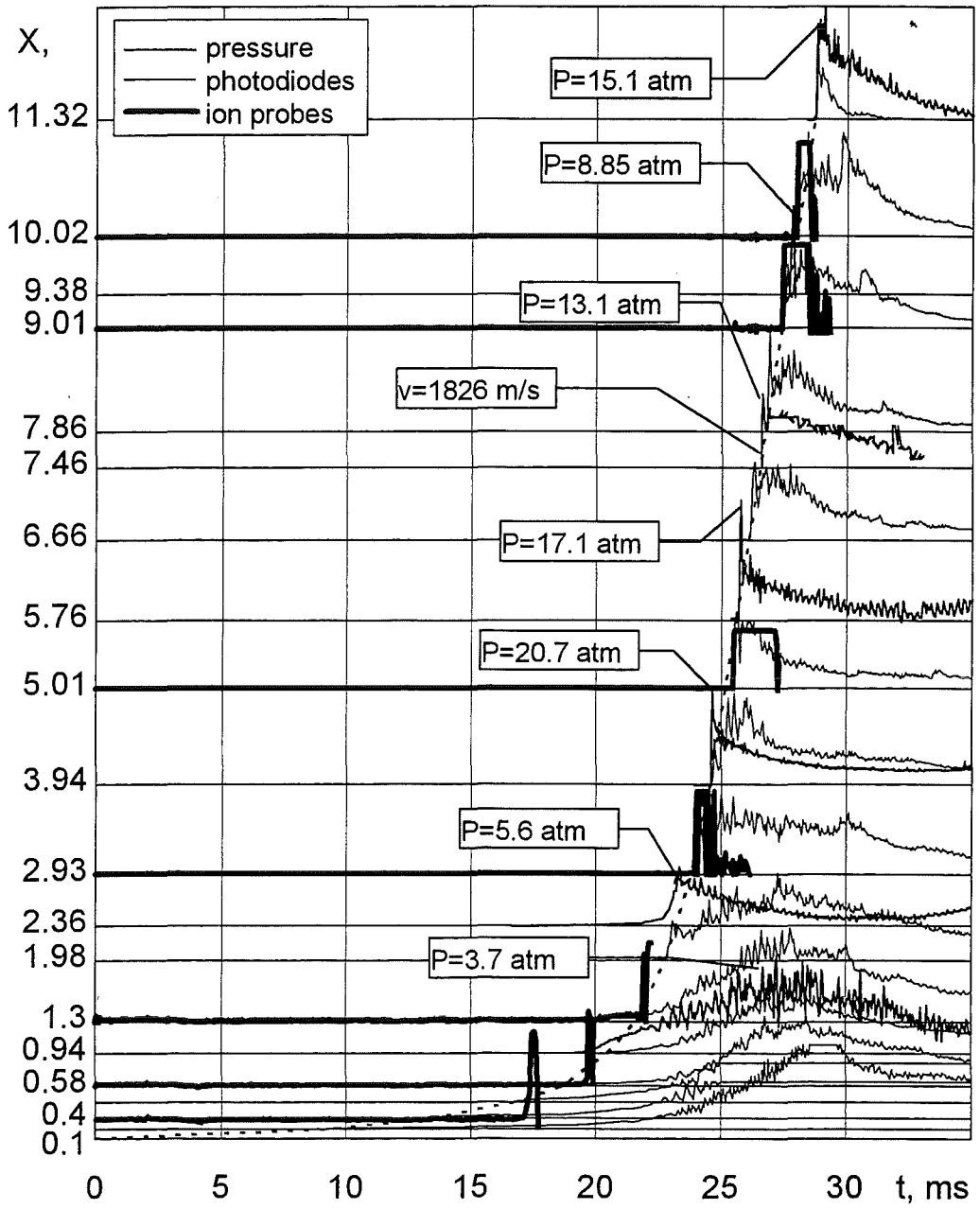

Figure 12: X-t diagram of flame propagation (quasi-detonation regime) in DRIVER tube (174 mm i. d.). Mixture: 60% H_2/air, BR = 0.3

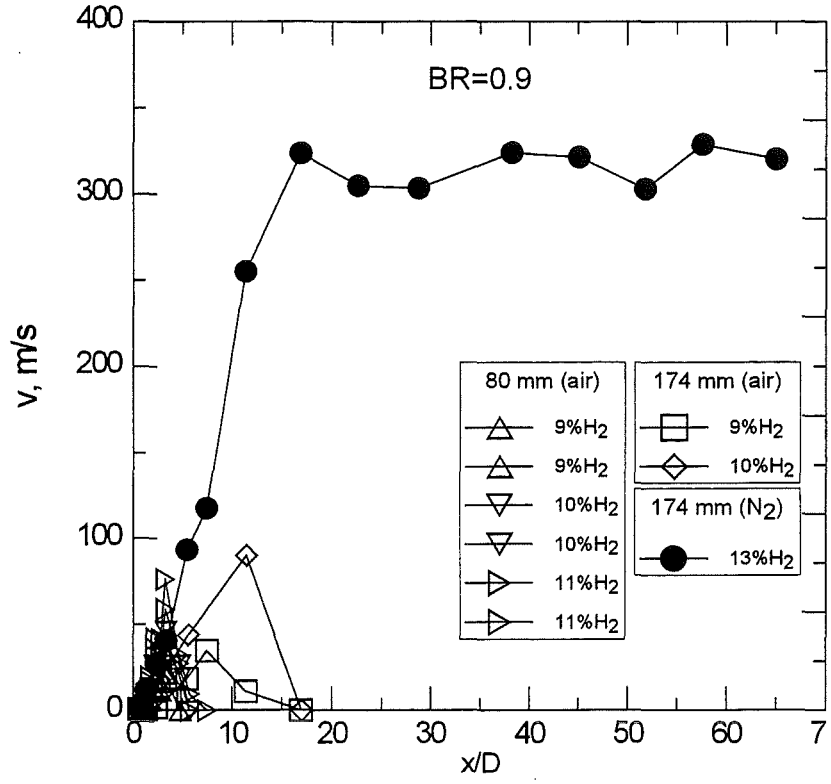

Figure 13: Flame velocities for lean hydrogen - air and $H_2/O_2/N_2$ mixtures versus dimensionless distance along tubes (BR = 0.9).

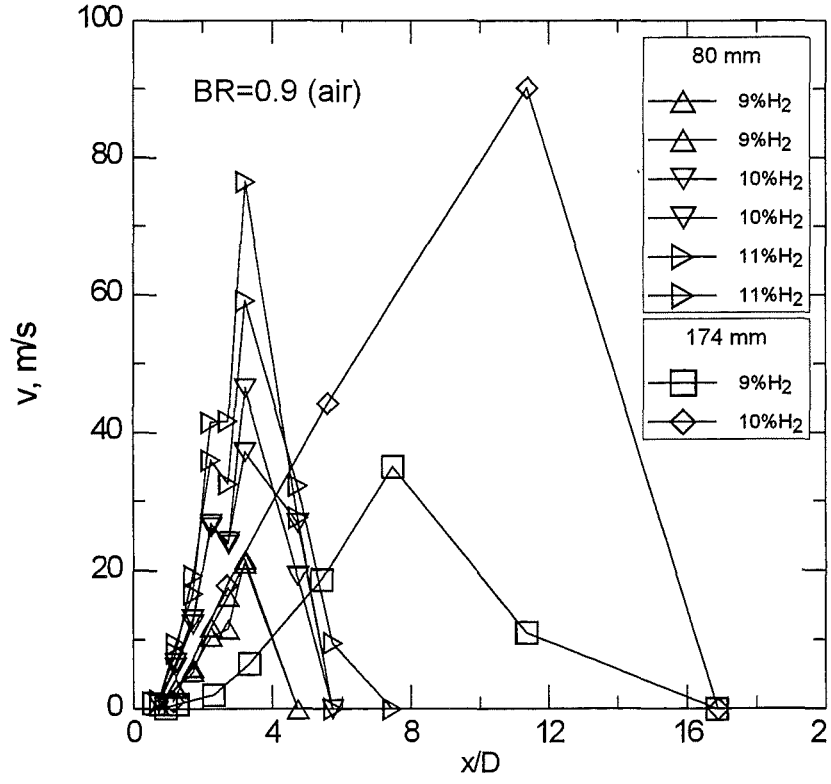

Figure 14: Flame velocities for lean hydrogen - air mixtures versus dimensionless distance along tubes (BR = 0.9) Expanded view for slow combustion regimes.

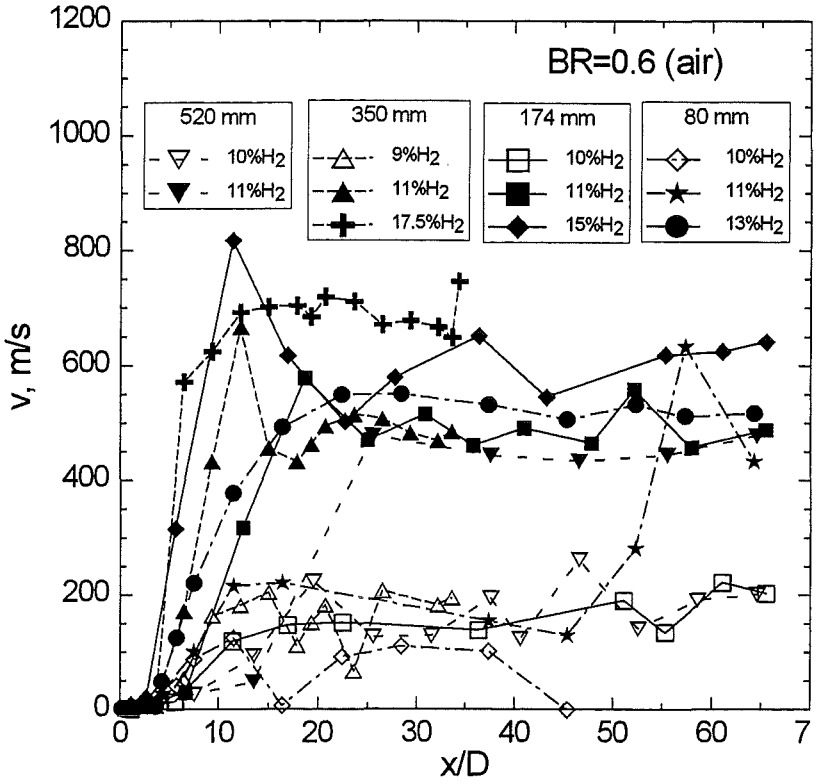

Figure 15: Flame velocities for lean hydrogen - air mixtures versus dimensionless distance along tubes (BR = 0.6).

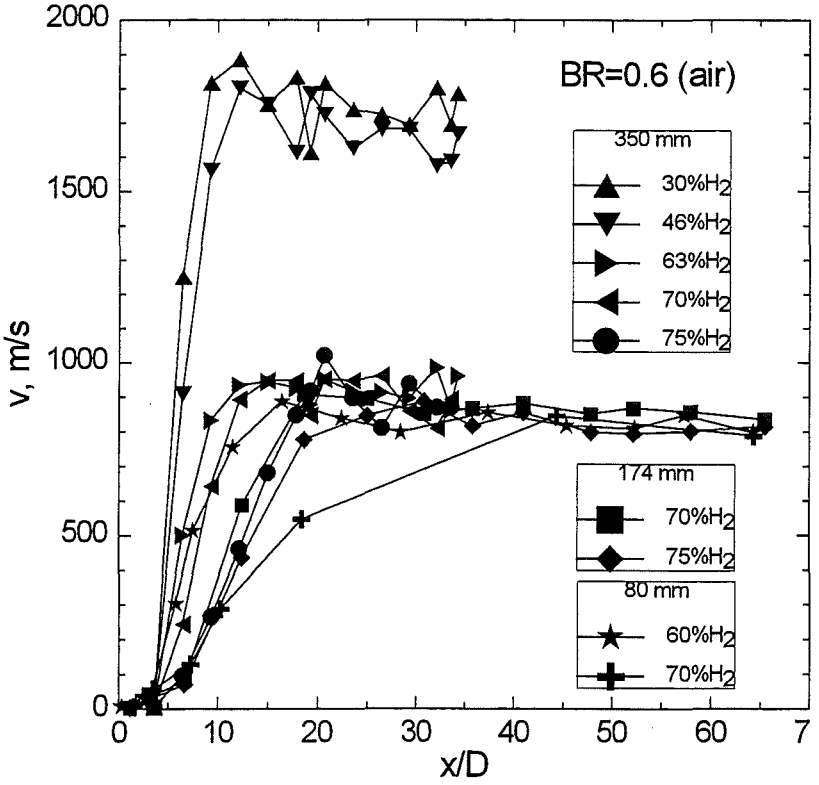

Figure 16: Flame velocities for rich hydrogen - air mixtures versus dimensionless distance along tubes (BR = 0.6).

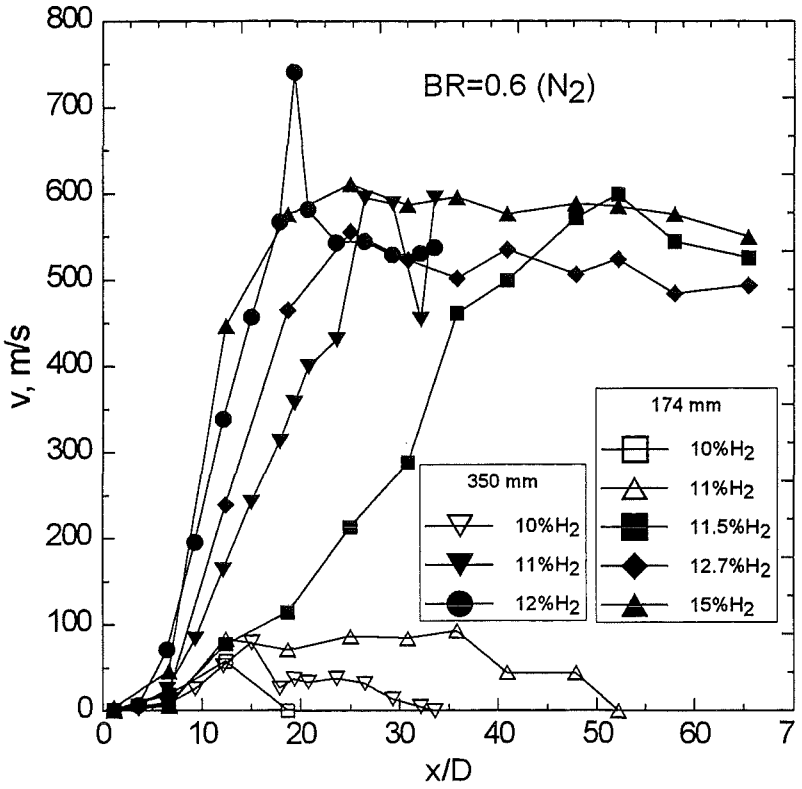

Figure 17: Flame velocities for stoichiometric H_2/O_2 mixtures diluted with N_2 versus dimensionless distance along the tube (BR = 0.6).

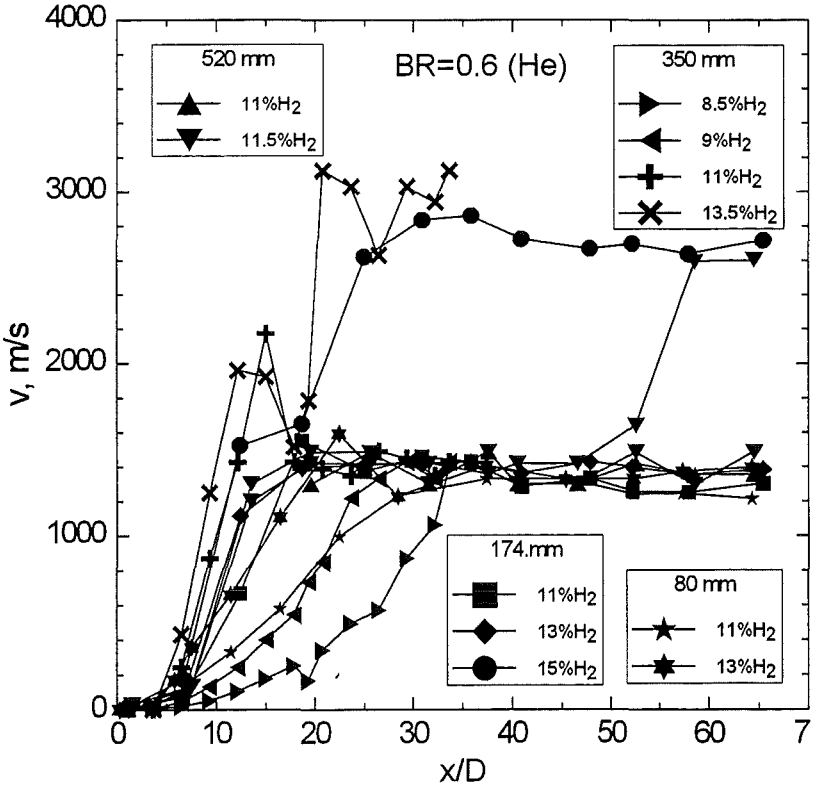

Figure 18: Flame velocities for stoichiometric H_2/O_2 mixtures diluted with He versus dimensionless distance along the tube (BR = 0.6).

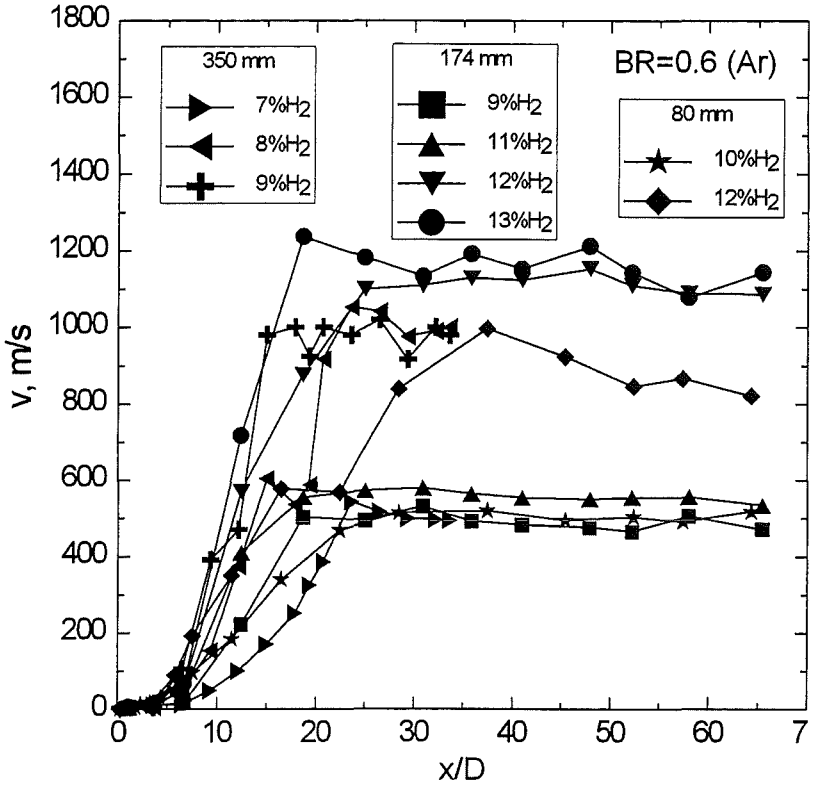

Figure 19: Flame velocities for stoichiometric H_2/O_2 mixtures diluted with Ar versus dimensionless distance along the tube (BR = 0.6).

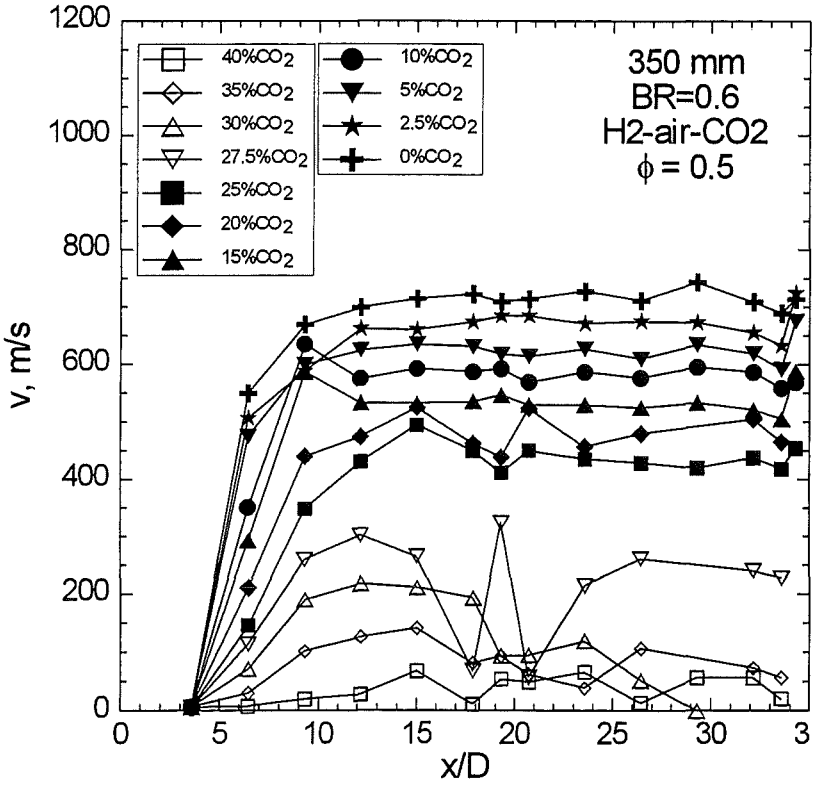

Figure 20: Flame velocities for H_2-air mixtures (equivalence ratio $\phi = 0.5$) diluted with CO_2 versus dimensionless distance along the tube (BR = 0.6).

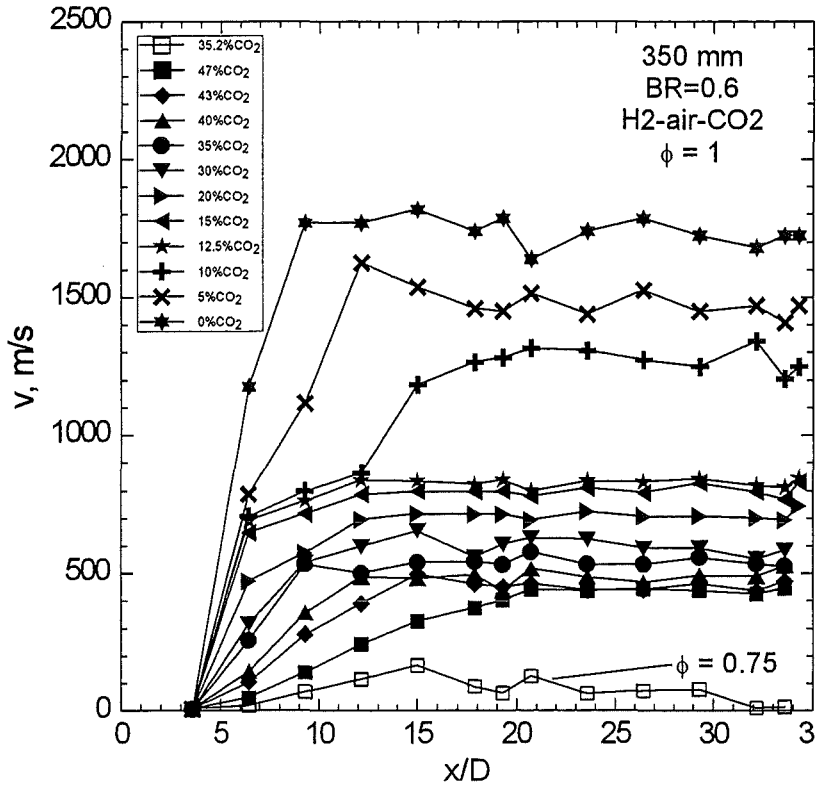

Figure 21: Flame velocities for nearly-stoichiometric H_2-air mixtures (equivalence ratio $\phi = 1$ and $\phi = 0.75$) diluted with CO_2 versus dimensionless distance along the tube (BR = 0.6).

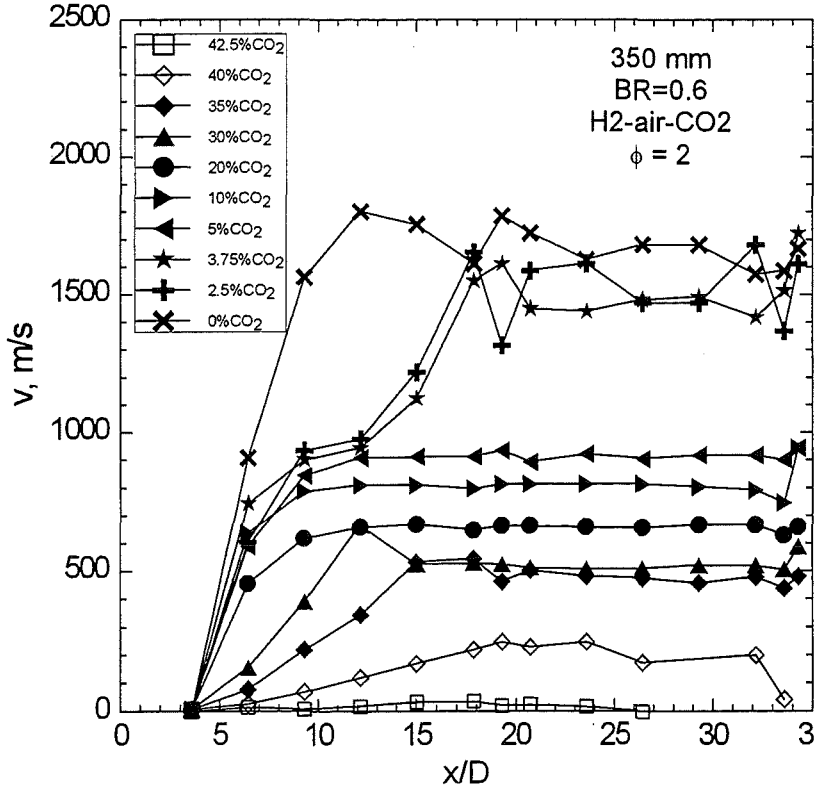

Figure 22: Flame velocities for rich H_2-air mixtures (equivalence ratio $\phi = 2$) diluted with CO_2 versus dimensionless distance along the tube (BR = 0.6).

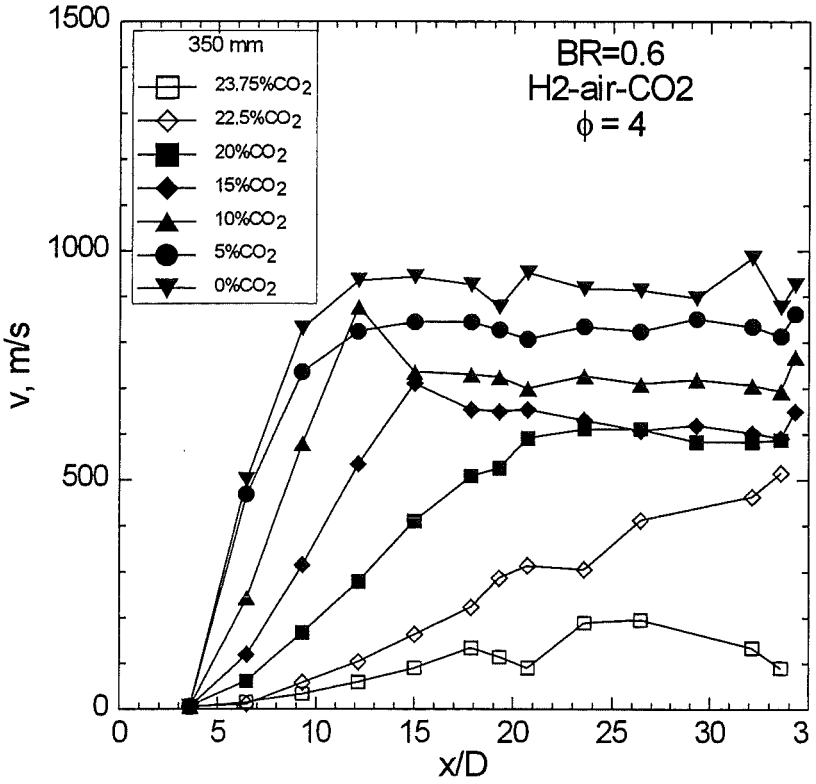

Figure 23: Flame velocities for rich H_2-air mixtures (equivalence ratio $\phi = 4$) diluted with CO_2 versus dimensionless distance along the tube (BR = 0.6).

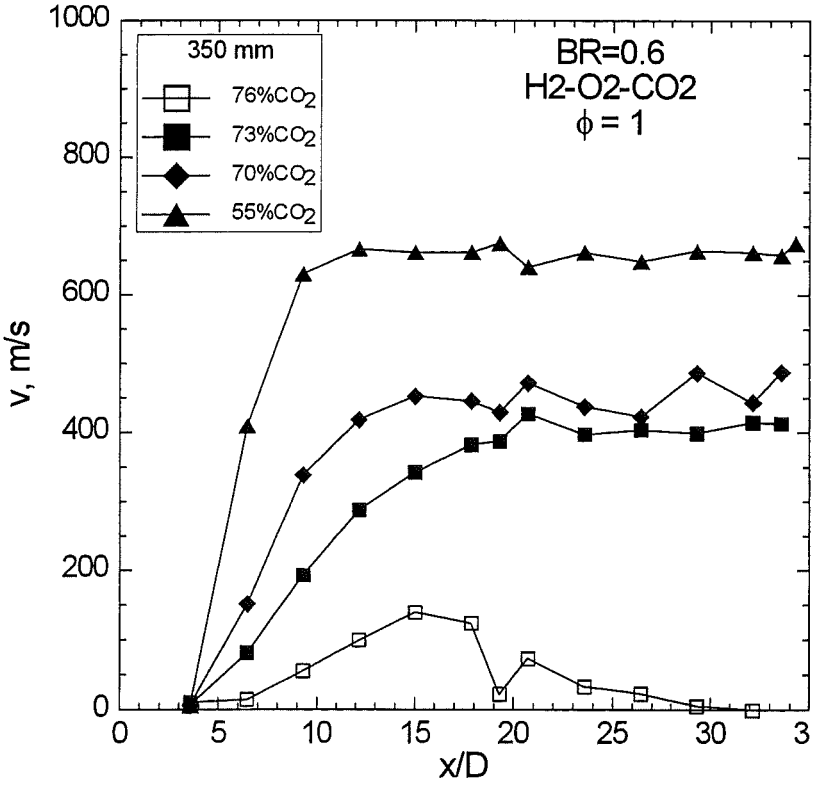

Figure 24: Flame velocities for stoichiometric H_2/O_2 mixtures (equivalence ratio ϕ = 1) diluted with CO_2 versus dimensionless distance along the tube (BR = 0.6).

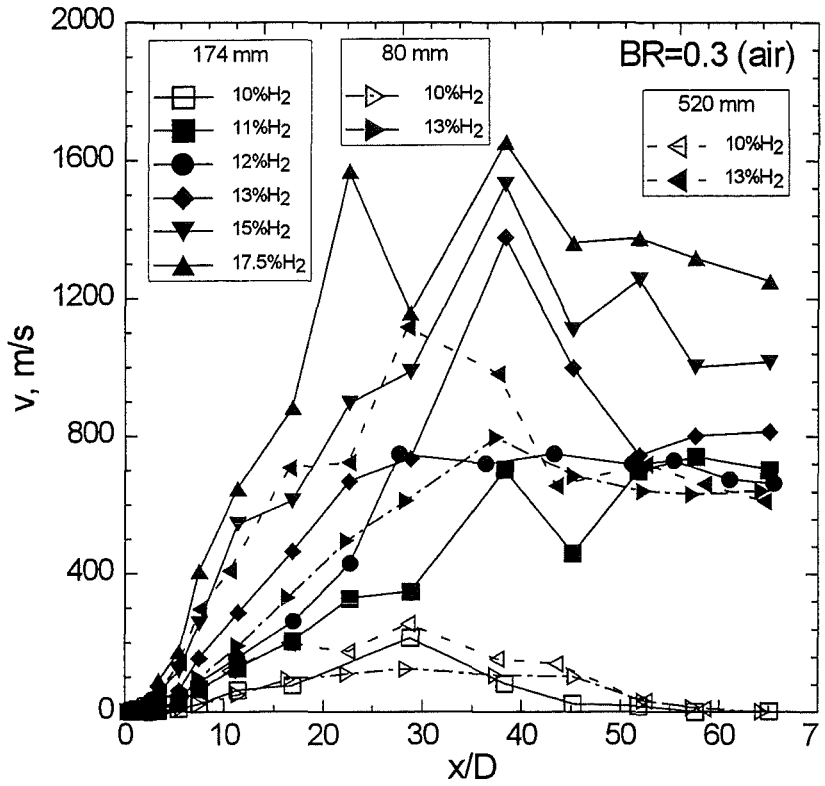

Figure 25: Flame velocities for lean hydrogen - air mixtures versus dimensionless distance along tubes (BR = 0.3).

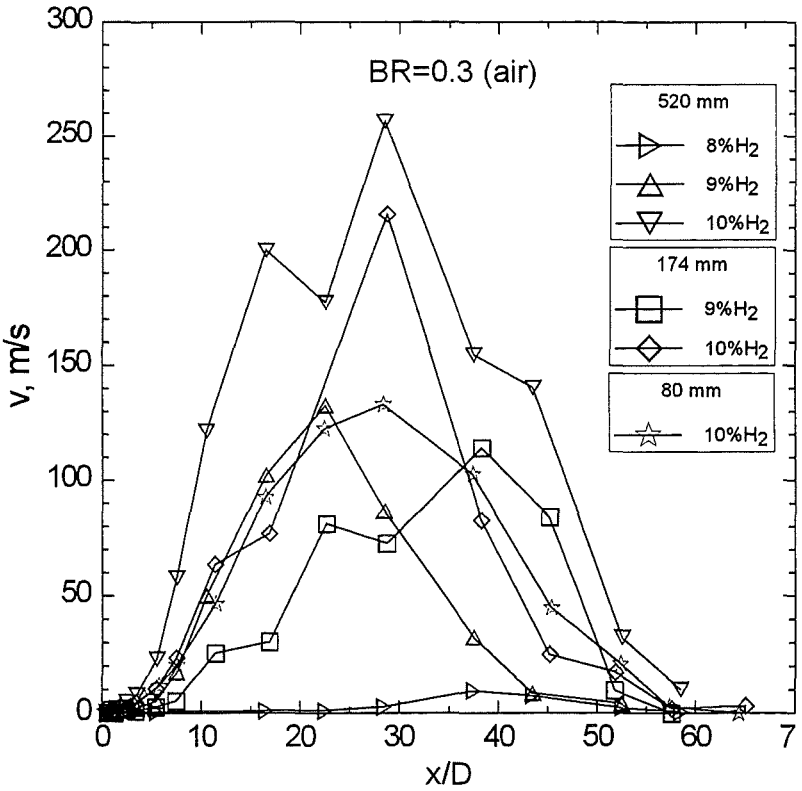

Figure 26: Flame velocities for lean hydrogen - air mixtures versus dimensionless distance along tubes (BR = 0.6) Expanded view for slow combustion regimes.

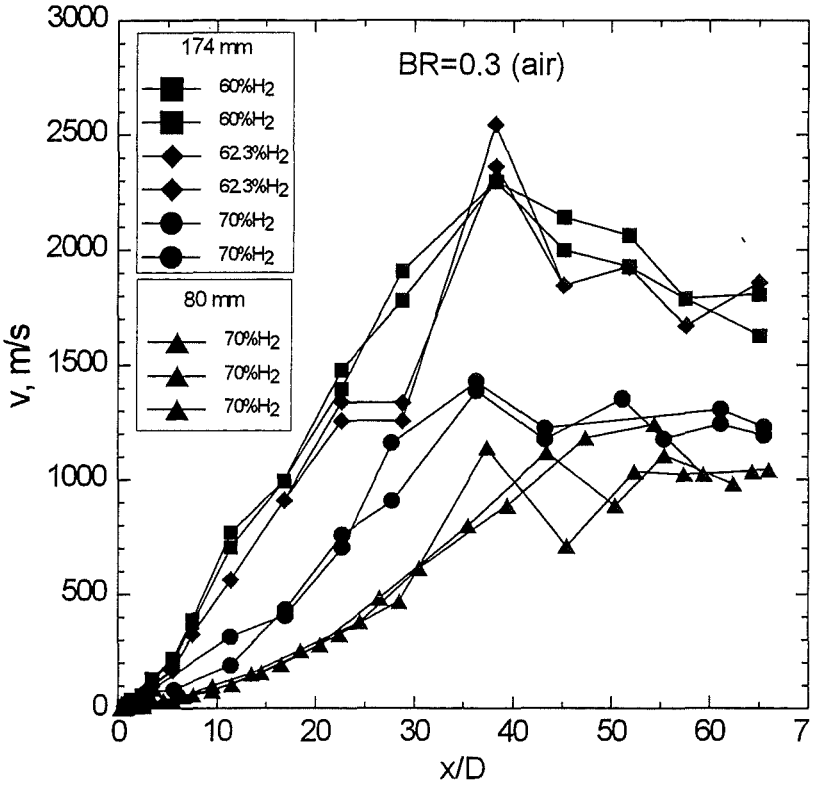

Figure 27: Flame velocities for rich hydrogen - air mixtures versus dimensionless distance along tubes (BR = 0.3).

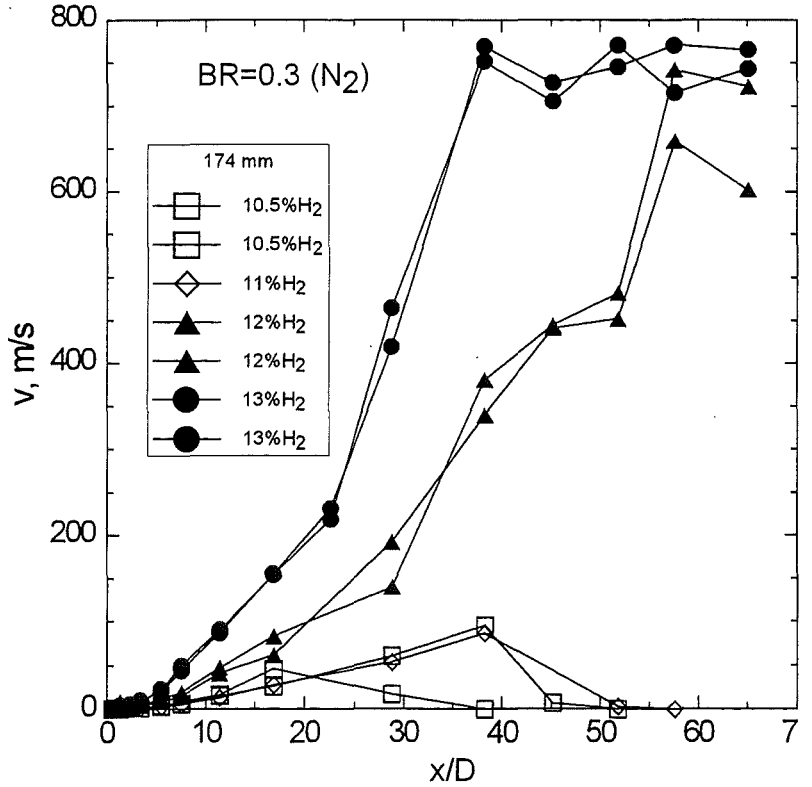

Figure 28: Flame velocities for stoichiometric H_2/O_2 mixtures diluted with N_2 versus dimensionless distance along the tube (BR = 0.3).

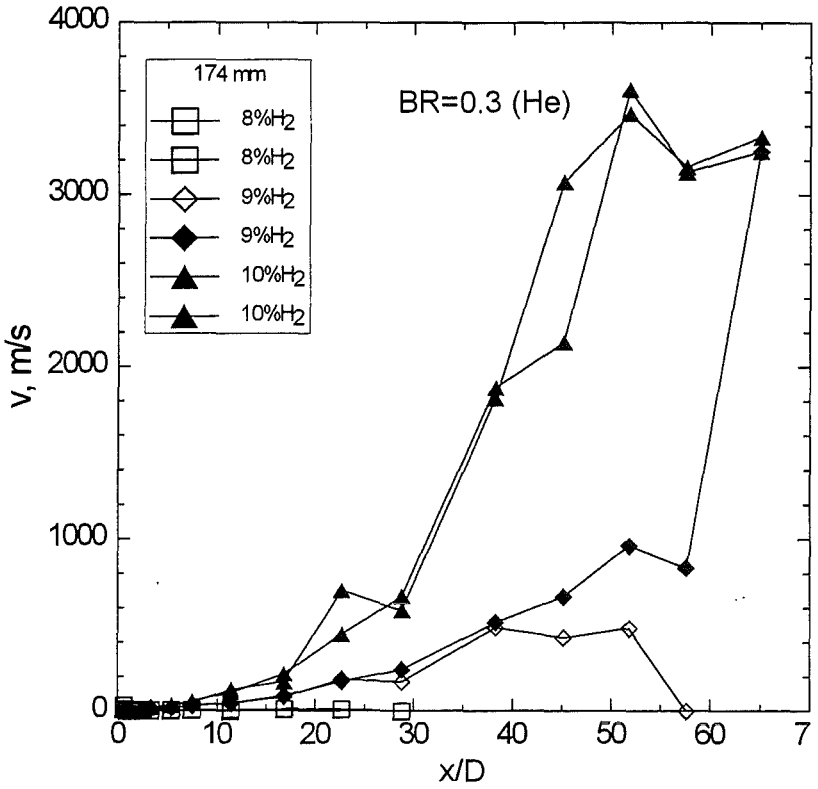

Figure 29: Flame velocities for stoichiometric H_2/O_2 mixtures diluted with He versus dimensionless distance along the tube (BR = 0.3).

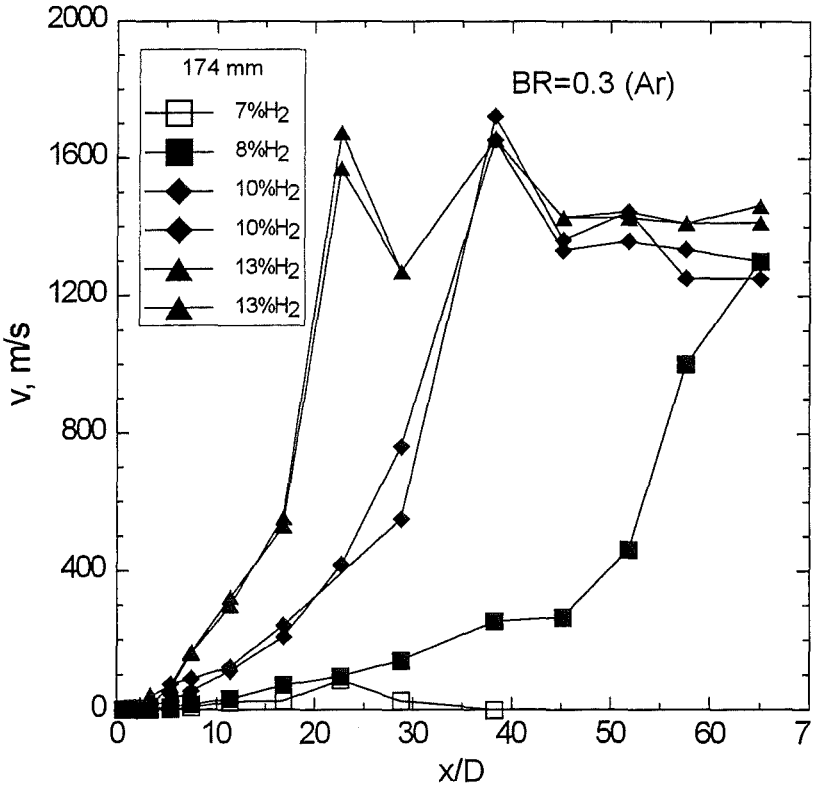

Figure 30: Flame velocities for stoichiometric H_2/O_2 mixtures diluted with Ar versus dimensionless distance along the tube (BR = 0.3).

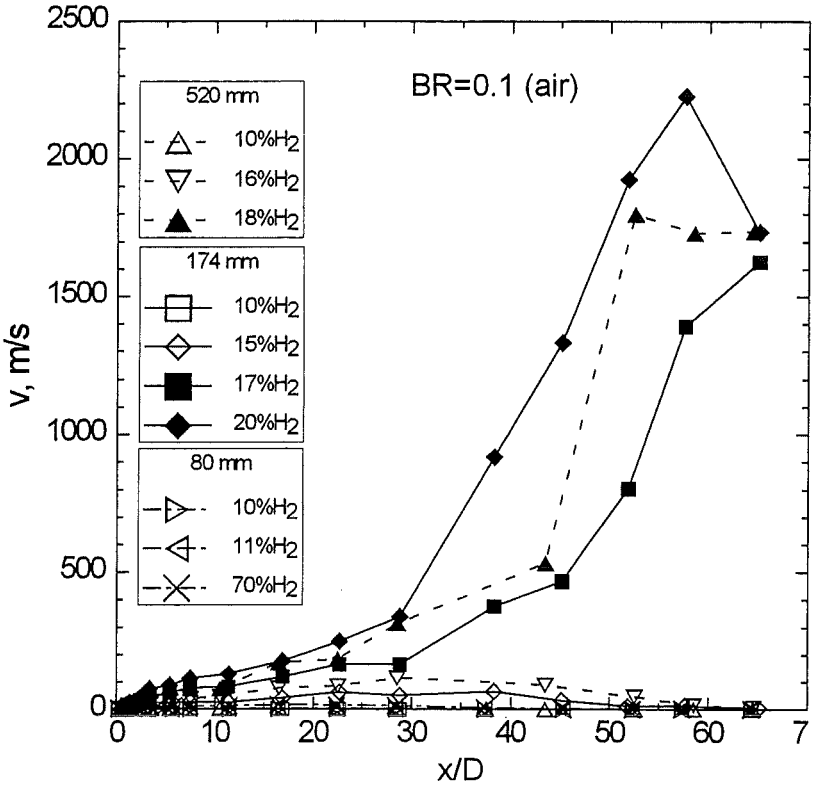

Figure 31: Flame velocities for lean hydrogen - air mixtures versus dimensionless distance along tubes (BR = 0.1).

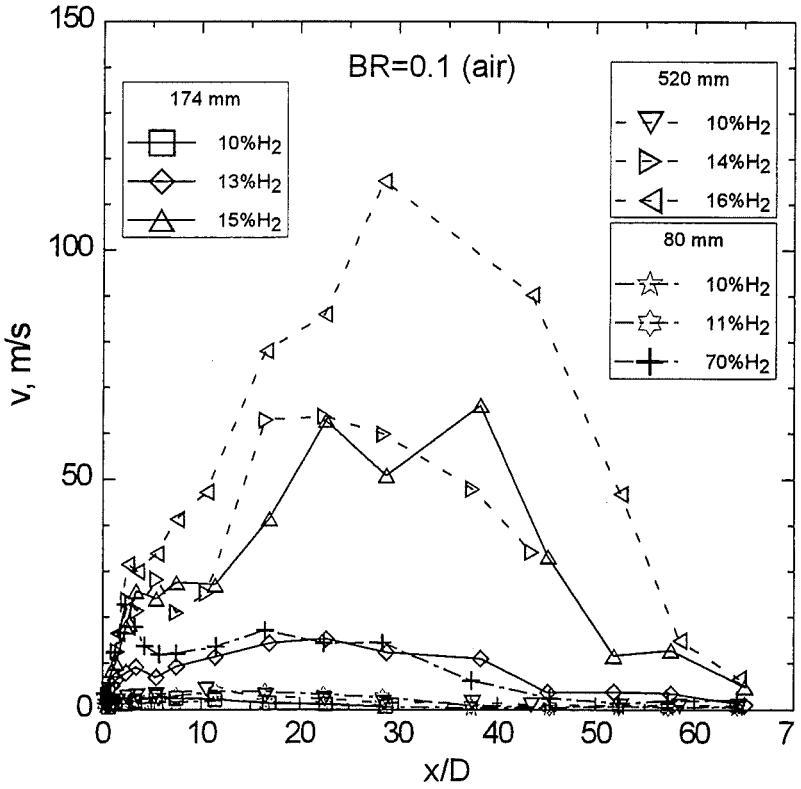

Figure 32: Flame velocities for lean hydrogen - air mixtures versus dimensionless distance along tubes (BR = 0.1). Expanded view for slow combustion regimes.

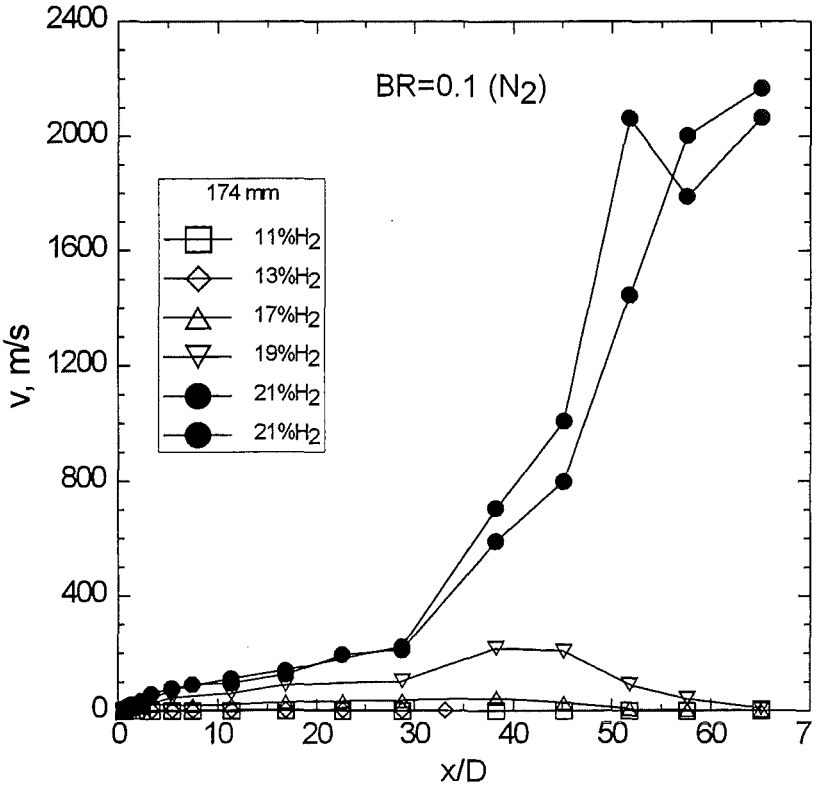

Figure 33: Flame velocities for stoichiometric H_2/O_2 mixtures diluted with N_2 versus dimensionless distance along the tube (BR = 0.1).

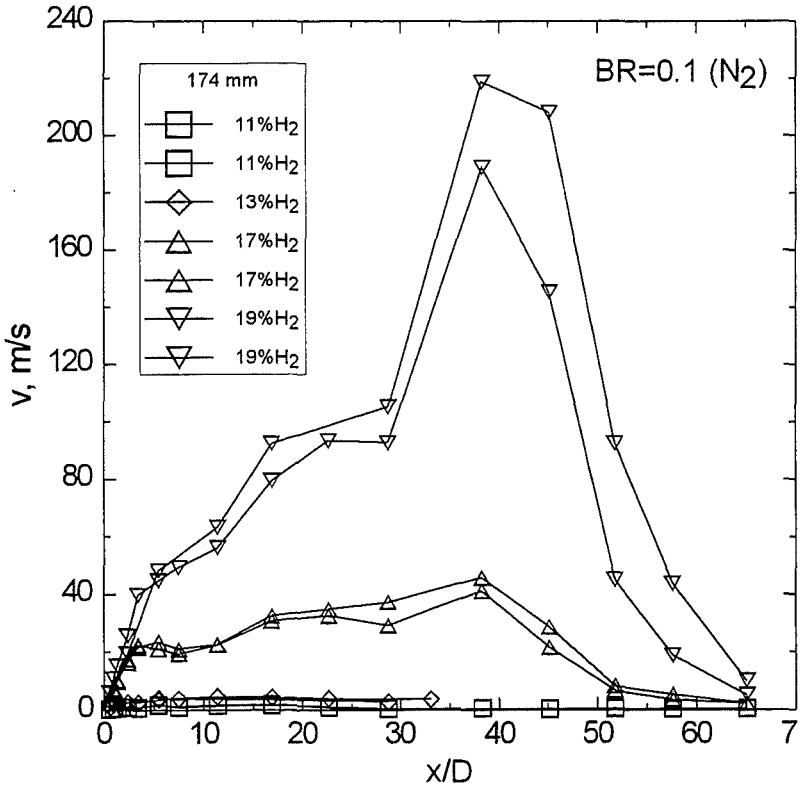

Figure 34: Flame velocities for stoichiometric H_2/O_2 mixtures diluted with N_2 versus dimensionless distance along the tube (BR = 0.1). Expanded view for slow combustion regimes.

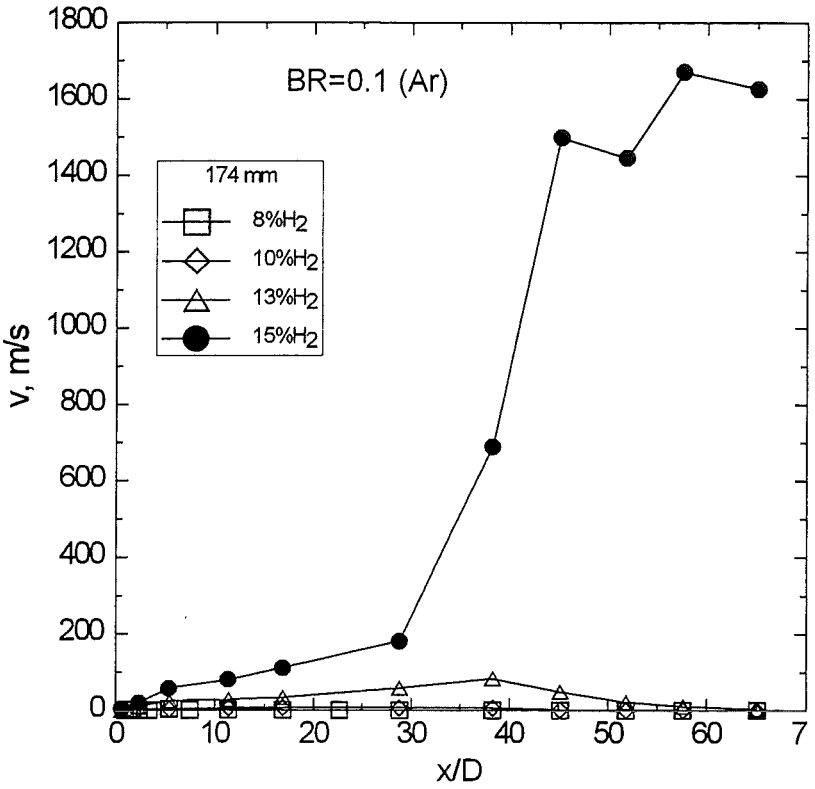

Figure 35: Flame velocities for stoichiometric H_2/O_2 mixtures diluted with Ar versus dimensionless distance along the tube (BR = 0.1).

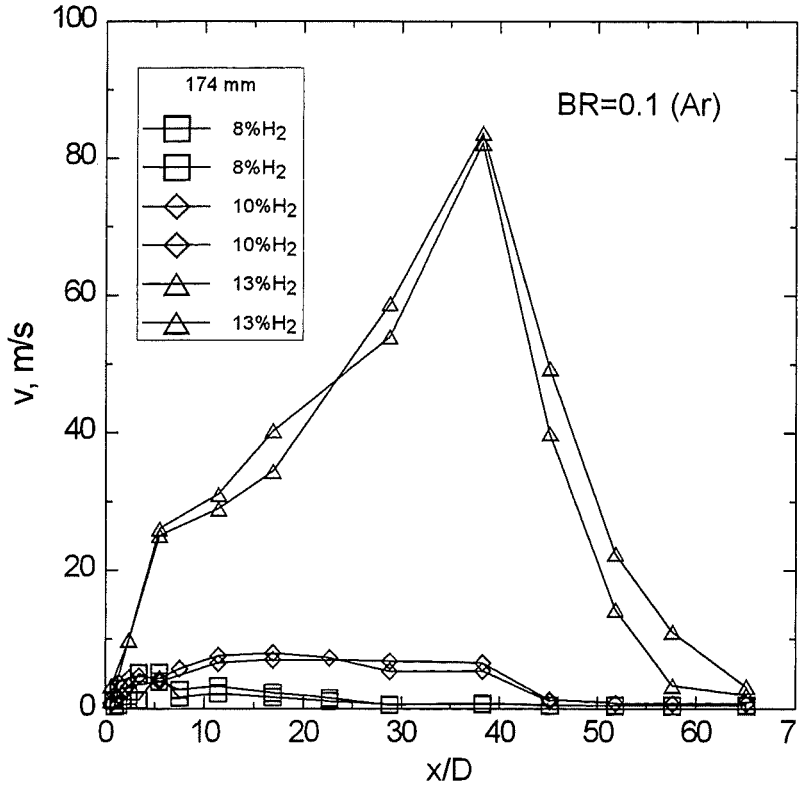

Figure 36: Flame velocities for stoichiometric H_2/O_2 mixtures diluted with Ar versus dimensionless distance along the tube (BR = 0.1). Expanded view for slow combustion regimes.

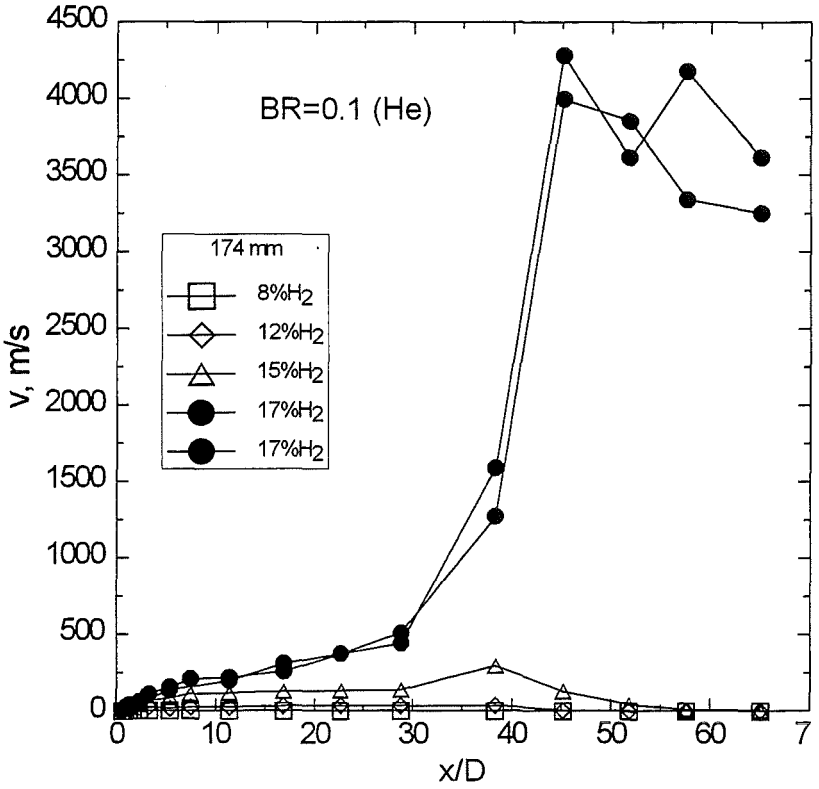

Figure 37: Flame velocities for stoichiometric H_2/O_2 mixtures diluted with He versus dimensionless distance along the tube (BR = 0.1).

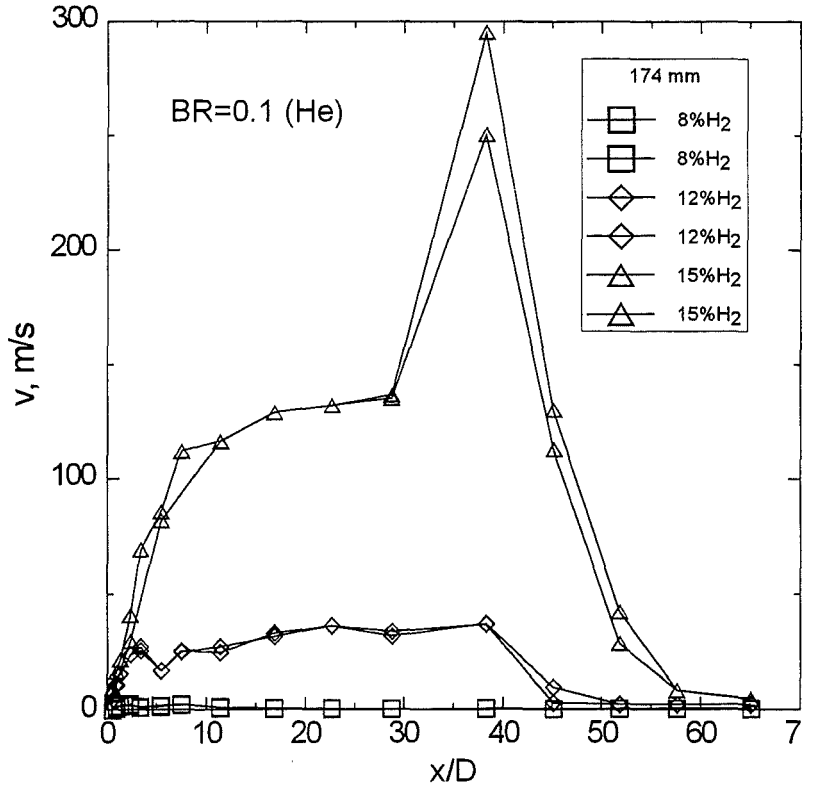

Figure 38: Flame velocities for stoichiometric H_2/O_2 mixtures diluted with He versus dimensionless distance along the tube (BR = 0.1). Expanded view for slow combustion regimes.

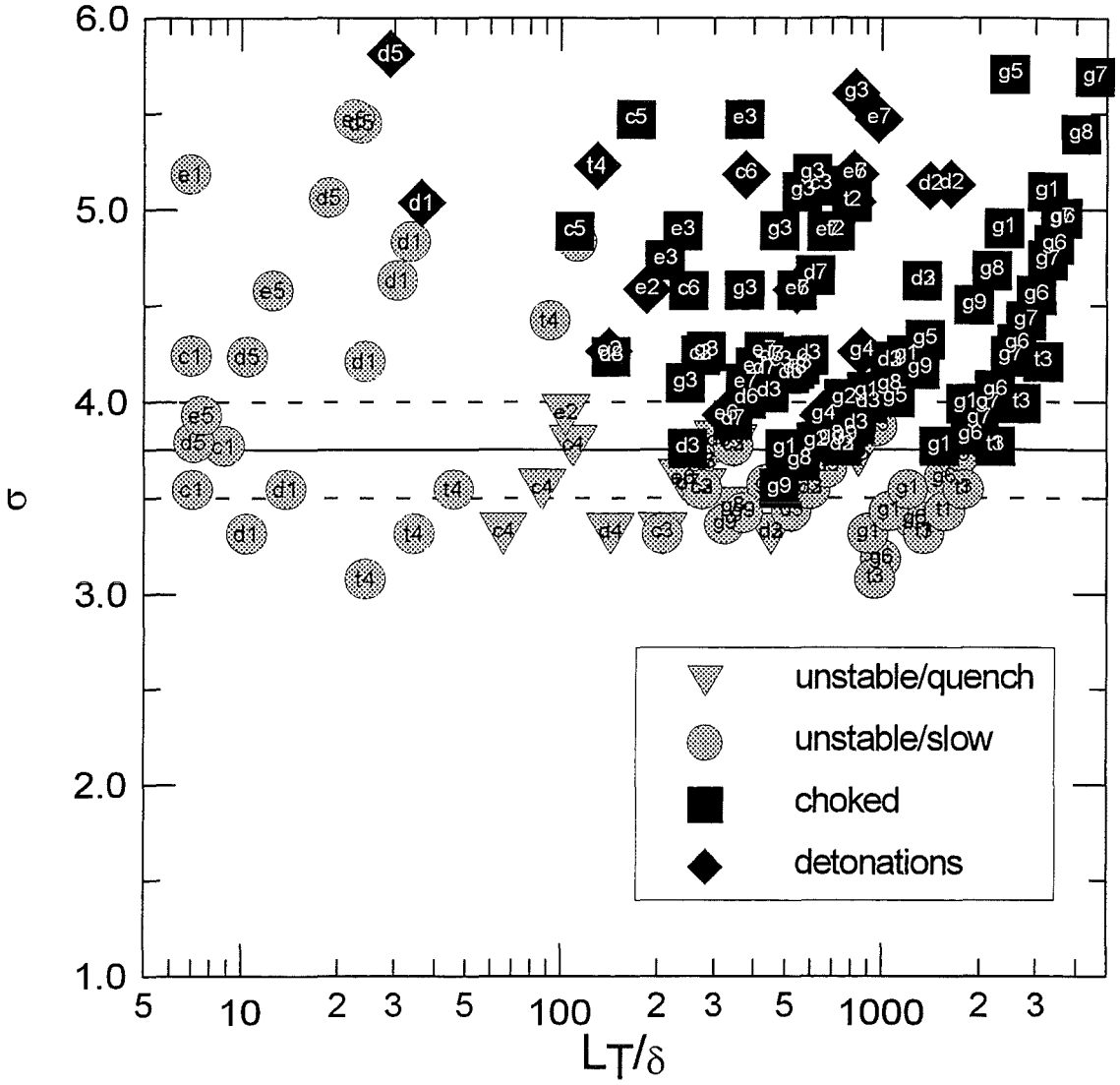

Figure 39: Resulting combustion regimes as a function of mixture expansion ratio σ and scale ratio L_T/δ. Data of all tests. Points are marked according to labels in Tables 1 - 4. Lines show critical value of $\sigma = 3.75 \pm 0.25$ for effective flame acceleration.

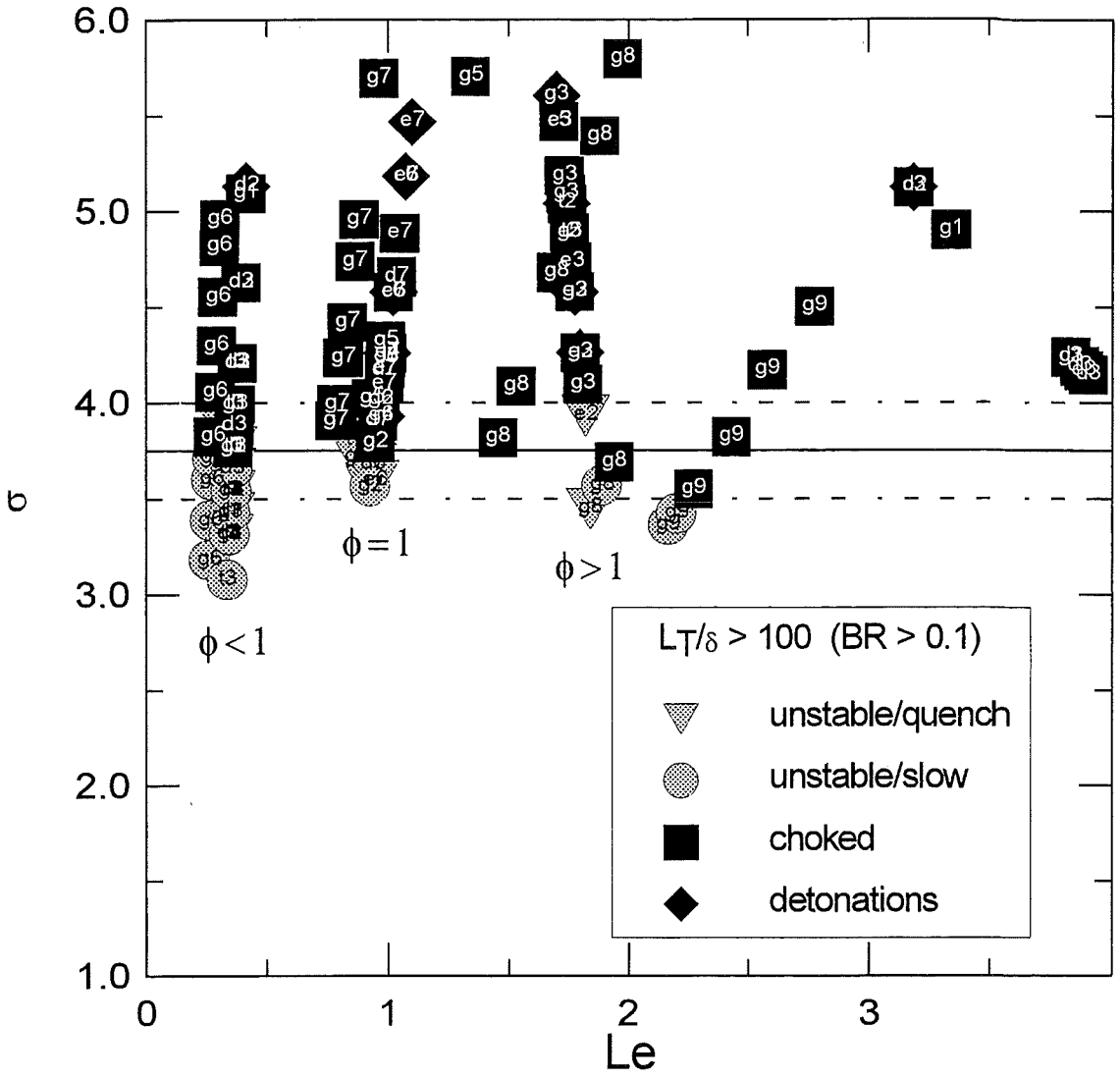

Figure 40: Resulting combustion regimes as a function of mixture expansion ratio σ and Lewis number Le. Data of tests with BR > 0.1. Points are marked according to labels in Tables 1 - 4. Lines show critical value of $\sigma = 3.75 \pm 0.25$ for effective flame acceleration. Equivalence ratio $\phi < 1$ for H_2-lean mixtures, $\phi = 1$ for stoichiometric ones, and $\phi > 1$ for H_2-rich mixtures.

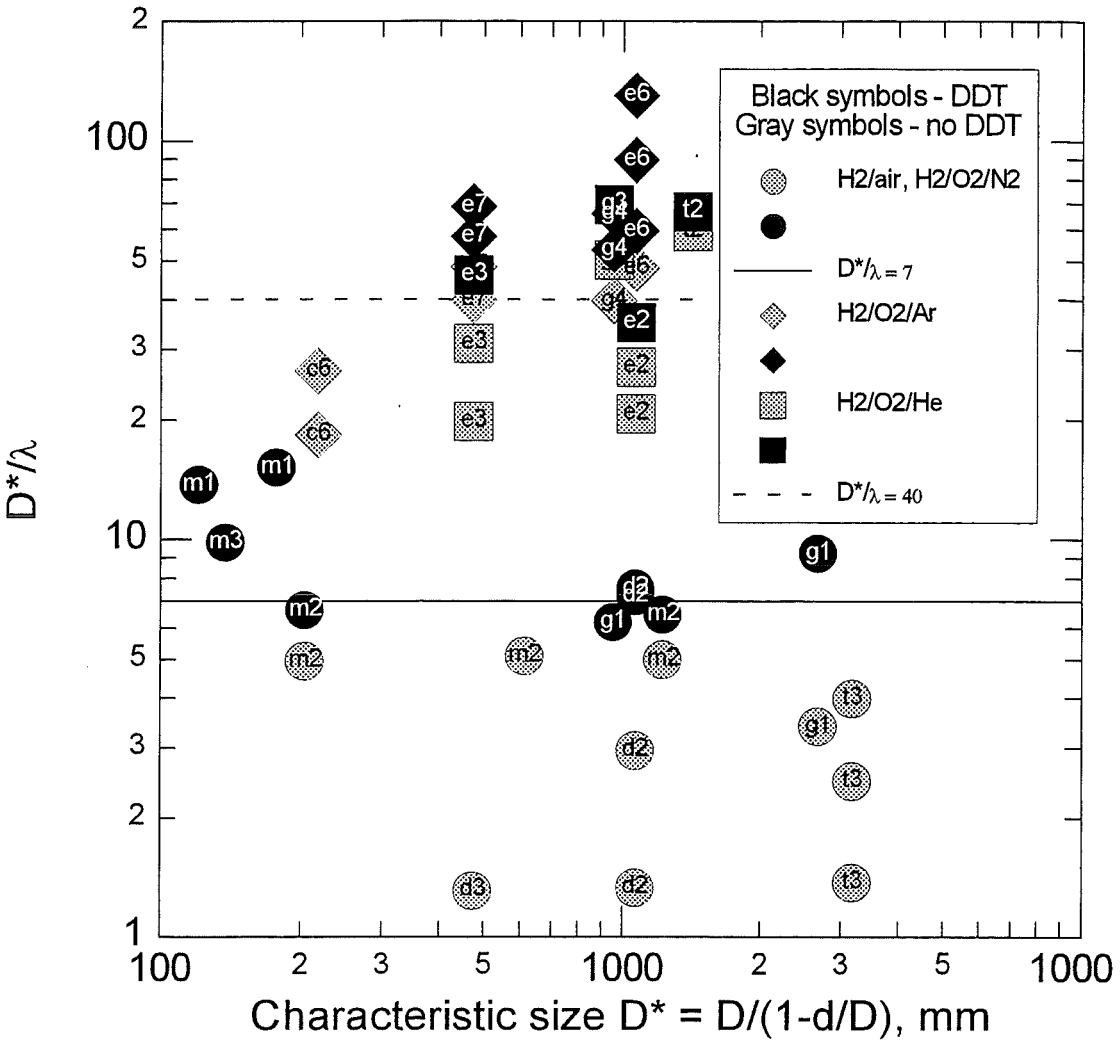

Figure 41: Critical conditions for onset of detonation in obstructed channels. Data points labeled with 'm1', 'm2', and 'm3' are from Refs. [15], [11], and [14] correspondingly. Other labels are given in Tables 1-4.

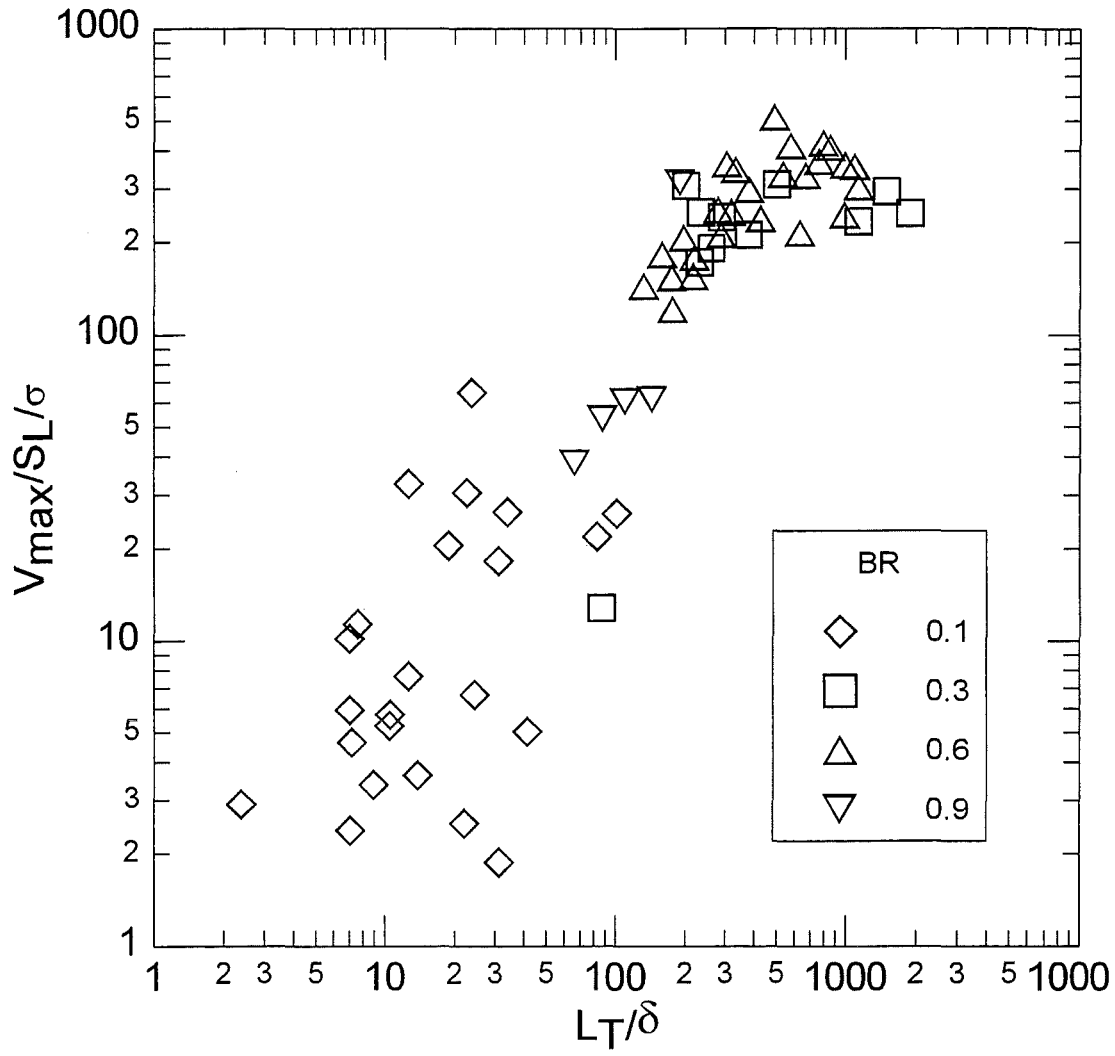

Figure 42: Reduced maximum visible flame speed $V_{max}/\sigma/S_L$ for slow combustion regimes as a function of scale ratio L_T/δ.

Table 1: Mixture properties and results of 80-mm channel experiments

Mixture	Label	BR	%H_2	ϕ	γ_r	S_L, m/s	δ_T, mm	c_{sr}, m/s	c_{sp}, m/s	σ	Le	β	L_T/δ	1000 S_L/c_{sr}	% of fuel consumed	Results
H_2/air	c1	0.1	10	0.26	1.40	0.25	0.29	360	660	3.54	0.35	6.6	7	0.68	82	Unstable/slow
H_2/air	c1	0.1	11	0.29	1.40	0.33	0.23	360	680	3.77	0.36	6.3	8	0.92	80-82	Unstable/slow
H_2/air	c1	0.1	70	5.55	1.40	0.91	0.29	580	1170	4.24	3.83	10.4	7	1.55	85-87	Unstable/slow
H_2/air	c2	0.3	10	0.26	1.40	0.25	0.29	360	660	3.54	0.35	6.6	280	0.68	71-72	Unstable/quench
H_2/air	c2	0.3	10	0.26	1.40	0.25	0.29	360	660	3.54	0.35	6.6	280	0.68	73-75	Unstable/slow
H_2/air	c2	0.3	11	0.29	1.40	0.33	0.23	360	680	3.77	0.36	6.3	350	0.92	80-81	Unstable/slow
H_2/air	c2	0.3	13	0.36	1.40	0.54	0.16	370	720	4.21	0.38	5.8	490	1.47	83-85	Choked flame
H_2/air	c2	0.3	70	5.55	1.40	0.91	0.29	580	1170	4.24	3.83	10.4	270	1.55	85-86	Choked flame
H_2/air	c3	0.6	9	0.24	1.40	0.17	0.38	360	640	3.31	0.34	6.9	210	0.48	23-37	Unstable/quench
H_2/air	c3	0.6	9	0.24	1.40	0.17	0.38	360	640	3.31	0.34	6.9	210	0.48	43-54	Unstable/slow
H_2/air	c3	0.6	10	0.26	1.40	0.25	0.29	360	660	3.54	0.35	6.6	280	0.68	25-42	Unstable/quench
H_2/air	c3	0.6	10	0.26	1.40	0.25	0.29	360	660	3.54	0.35	6.6	280	0.68	46-57	Unstable/slow
H_2/air	c3	0.6	11	0.29	1.40	0.33	0.23	360	680	3.77	0.36	6.3	350	0.92	36	Unstable/quench
H_2/air	c3	0.6	11	0.29	1.40	0.33	0.23	360	680	3.77	0.36	6.3	350	0.92	70-76	Unstable/slow
H_2/air	c3	0.6	13	0.36	1.40	0.54	0.16	370	720	4.21	0.38	5.8	490	1.47	80	Choked flame
H_2/air	c3	0.6	60	3.57	1.40	2.13	0.12	520	1130	5.12	3.19	8.9	650	4.11	86	Choked flame
H_2/air	c3	0.6	70	5.55	1.40	0.91	0.29	580	1170	4.24	3.83	10.4	270	1.55	83-85	Choked flame
H_2/air	c4	0.9	9	0.24	1.40	0.17	0.38	360	640	3.31	0.34	6.9	66	0.48	2-2.2	Unstable/quench
H_2/air	c4	0.9	10	0.26	1.40	0.25	0.29	360	660	3.54	0.35	6.6	87	0.68	2.3-2.8	Unstable/quench
H_2/air	c4	0.9	11	0.29	1.40	0.33	0.23	360	680	3.77	0.36	6.3	110	0.92	2.9-3.0	Unstable/quench
H_2/O_2/He	c5	0.6	11	1.00	1.61	0.59	0.73	860	1850	4.89	1.75	6.5	110	0.69	82	Choked flame
H_2/O_2/He	c5	0.6	13	1.00	1.60	0.98	0.47	840	1900	5.47	1.71	5.9	170	1.17	83	Choked flame
H_2/O_2/Ar	c6	0.6	10	1.00	1.61	0.23	0.32	330	690	4.58	1.02	6.3	250	0.69	78	Choked flame
H_2/O_2/Ar	c6	0.6	12	1.00	1.60	0.39	0.21	330	740	5.18	1.07	5.7	380	1.18	83	Choked flame

Table 2: Mixture properties and results of 174-mm tube experiments

Mixture	Label	BR	%H_2	ϕ	γ_r	S_L, m/s	δ_T, mm	c_{sr}, m/s	c_{sp}, m/s	σ	Le	β	L_T/δ	1000 S_L/c_{sr}	% of fuel consumed	Results
H_2/air	d1	0.09	9	0.24	1.40	0.17	0.38	360	640	3.31	0.34	6.9	10	0.48	79-82	Unstable/slow
H_2/air	d1	0.09	10	0.26	1.40	0.25	0.29	360	660	3.54	0.35	6.6	13	0.68	78-85	Unstable/slow
H_2/air	d1	0.09	13	0.36	1.40	0.54	0.16	370	720	4.21	0.38	5.8	23	1.47	87	Unstable/slow
H_2/air	d1	0.09	15	0.42	1.40	0.78	0.13	370	760	4.63	0.39	5.3	29	2.11	88	Unstable/slow
H_2/air	d1	0.09	16	0.45	1.40	0.91	0.12	370	780	4.83	0.40	5.2	32	2.44	88	Unstable/slow
H_2/air	d1	0.09	17	0.49	1.40	1.04	0.11	370	800	5.03	0.41	5.0	35	2.79	88	Detonation
H_2/air	d1	0.09	20	0.60	1.40	1.46	0.09	380	860	5.60	0.44	4.5	41	3.83	85-87	Detonation
H_2/air	d2	0.3	9	0.24	1.40	0.17	0.38	360	640	3.31	0.34	6.9	450	0.48	59-61	Unstable/quench
H_2/air	d2	0.3	9	0.24	1.40	0.17	0.38	360	640	3.31	0.34	6.9	450	0.48	61-69	Unstable/quench
H_2/air	d2	0.3	10	0.26	1.40	0.25	0.29	360	660	3.54	0.35	6.6	600	0.68	73-77	Unstable/slow
H_2/air	d2	0.3	10	0.26	1.40	0.25	0.29	360	660	3.54	0.35	6.6	600	0.68	65	Unstable/quench
H_2/air	d2	0.3	10	0.26	1.40	0.25	0.29	360	660	3.54	0.35	6.6	600	0.68	81-85	Unstable/slow
H_2/air	d2	0.3	10	0.26	1.40	0.25	0.29	360	660	3.54	0.35	6.6	600	0.68	71-85	Unstable/slow
H_2/air	d2	0.3	10	0.26	1.40	0.25	0.29	360	660	3.54	0.35	6.6	600	0.68	55-65	Unstable/quench
H_2/air	d2	0.3	11	0.29	1.40	0.33	0.23	360	680	3.77	0.36	6.3	750	0.92	77	Choked flame
H_2/air	d2	0.3	11	0.29	1.40	0.33	0.23	360	680	3.77	0.36	6.3	750	0.92	76	Choked flame
H_2/air	d2	0.3	12	0.32	1.40	0.43	0.19	360	700	3.99	0.37	6.0	910	1.19	83	Choked flame
H_2/air	d2	0.3	13	0.36	1.40	0.54	0.16	370	720	4.21	0.38	5.8	1060	1.47	87-90	Choked flame
H_2/air	d2	0.3	15	0.42	1.40	0.78	0.13	370	760	4.63	0.39	5.3	1340	2.11	89	Choked flame
H_2/air	d2	0.3	17.5	0.50	1.40	1.11	0.11	380	810	5.13	0.42	4.9	1640	2.96	81-87	Quasi-detonation
H_2/air	d2	0.3	20	0.60	1.40	1.46	0.09	380	860	5.60	0.44	4.5	1870	3.83	96	Quasi-detonation
H_2/air	d2	0.3	60	3.57	1.40	2.13	0.12	520	1130	5.12	3.19	8.9	1410	4.11	86	Quasi-detonation
H_2/air	d2	0.3	60	3.57	1.40	2.13	0.12	520	1130	5.12	3.19	8.9	1410	4.11	86-87	Quasi-detonation
H_2/air	d2	0.3	62.32	3.94	1.40	1.85	0.14	530	1130	4.93	3.32	9.2	1220	3.49	82-83	Quasi-detonation
H_2/air	d2	0.3	70	5.55	1.40	0.91	0.29	580	1170	4.24	3.83	10.4	590	1.55	90-93	Choked flame

Table 2: (continued)

Mixture	Label	BR	%H_2	ϕ	γ_r	S_L, m/s	δ_T, mm	c_{sr}, m/s	c_{sp}, m/s	σ	Le	β	L_T/δ	1000 S_L/c_{sr}	% of fuel consumed	Results
H_2/air	d3	0.6	9	0.24	1.40	0.17	0.38	360	640	3.31	0.34	6.9	450	0.48	35-57	Unstable/quench
H_2/air	d3	0.6	9	0.24	1.40	0.17	0.38	360	640	3.31	0.34	6.9	450	0.48	13-24	Unstable/quench
H_2/air	d3	0.6	9.5	0.25	1.40	0.21	0.33	360	650	3.43	0.35	6.7	520	0.58	15	Unstable/quench
H_2/air	d3	0.6	9.5	0.25	1.40	0.21	0.33	360	650	3.43	0.35	6.7	520	0.58	47	Unstable/slow
H_2/air	d3	0.6	10	0.26	1.40	0.25	0.29	360	660	3.54	0.35	6.6	600	0.68	18	Unstable/quench
H_2/air	d3	0.6	10	0.26	1.40	0.25	0.29	360	660	3.54	0.35	6.6	600	0.68	15-18	Unstable/quench
H_2/air	d3	0.6	10	0.26	1.40	0.25	0.29	360	660	3.54	0.35	6.6	600	0.68	55-66	Unstable/slow
H_2/air	d3	0.6	10.5	0.28	1.40	0.29	0.26	360	670	3.66	0.36	6.4	680	0.80	65	Unstable/quench
H_2/air	d3	0.6	10.5	0.28	1.40	0.29	0.26	360	670	3.66	0.36	6.4	680	0.80	81-82	Unstable/slow
H_2/air	d3	0.6	11	0.29	1.40	0.33	0.23	360	680	3.77	0.36	6.3	750	0.92	70-81	Choked flame
H_2/air	d3	0.6	11.5	0.31	1.40	0.38	0.21	360	690	3.88	0.36	6.2	830	1.05	60-85	Choked flame
H_2/air	d3	0.6	12	0.32	1.40	0.43	0.19	360	700	3.99	0.37	6.0	910	1.19	75-83	Choked flame
H_2/air	d3	0.6	13	0.36	1.40	0.54	0.16	370	720	4.21	0.38	5.8	1060	1.47	74-76	Choked flame
H_2/air	d3	0.6	15	0.42	1.40	0.78	0.13	370	760	4.63	0.39	5.3	1340	2.11	71-73	Choked flame
H_2/air	d3	0.6	70	5.55	1.40	0.91	0.29	580	1170	4.24	3.83	10.4	590	1.55	69-89	Choked flame
H_2/air	d3	0.6	70.5	5.69	1.40	0.85	0.31	590	1170	4.19	3.86	10.5	560	1.44	87	Choked flame
H_2/air	d3	0.6	70.75	5.76	1.40	0.82	0.32	590	1170	4.17	3.88	10.5	540	1.39	83-85	Choked flame
H_2/air	d3	0.6	71	5.83	1.40	0.79	0.34	590	1170	4.14	3.90	10.6	520	1.34	84-85	Choked flame
H_2/air	d3	0.6	72	6.12	1.40	0.68	0.39	600	1170	4.05	3.97	10.8	450	1.13	85-92	Choked flame
H_2/air	d3	0.6	75	7.14	1.40	0.38	0.70	630	1190	3.76	4.20	11.4	250	0.60	87	Choked flame
H_2/air	d4	0.9	9	0.24	1.40	0.17	0.38	360	640	3.31	0.34	6.9	140	0.48	4.1	Unstable/quench
H_2/air	d4	0.9	10	0.26	1.40	0.25	0.29	360	660	3.54	0.35	6.6	190	0.68	14-19	Unstable/quench
$H_2/O_2/N_2$	d5	0.09	11	1.00	1.40	0.12	0.56	370	690	3.79	0.95	6.6	7	0.32	81	Unstable/slow
$H_2/O_2/N_2$	d5	0.09	13	1.00	1.40	0.20	0.38	370	730	4.23	0.99	6.1	10	0.53	83-85	Unstable/slow
$H_2/O_2/N_2$	d5	0.09	17	1.00	1.40	0.44	0.21	380	810	5.06	1.08	5.3	18	1.17	84-88	Unstable/slow
$H_2/O_2/N_2$	d5	0.09	19	1.00	1.40	0.62	0.17	380	850	5.45	1.12	4.9	23	1.63	84-85	Unstable/slow
$H_2/O_2/N_2$	d5	0.09	21	1.00	1.40	0.84	0.14	390	880	5.81	1.17	4.6	28	2.18	83	Detonation

Table 2: (continued)

Mixture	Label	BR	%H_2	ϕ	γ_r	S_L, m/s	δ_T, mm	c_{sr}, m/s	c_{sp}, m/s	σ	Le	β	L_T/δ	1000 S_L/c_{sr}	% of fuel consumed	Results
$H_2/O_2/N_2$	d6	0.3	10.5	1.00	1.40	0.10	0.62	370	680	3.68	0.93	6.8	280	0.28	75-76	Unstable/quench
$H_2/O_2/N_2$	d6	0.3	11	1.00	1.40	0.12	0.56	370	690	3.79	0.95	6.6	310	0.32	76	Unstable/quench
$H_2/O_2/N_2$	d6	0.3	12	1.00	1.40	0.15	0.46	370	710	4.01	0.97	6.4	380	0.42	81	Choked flame
$H_2/O_2/N_2$	d6	0.3	13	1.00	1.40	0.20	0.38	370	730	4.23	0.99	6.1	450	0.53	77-78	Choked flame
$H_2/O_2/N_2$	d7	0.6	10	1.00	1.40	0.09	0.70	360	670	3.56	0.92	6.9	250	0.24	6.7	Unstable/quench
$H_2/O_2/N_2$	d7	0.6	10.5	1.00	1.40	0.10	0.62	370	680	3.68	0.93	6.8	280	0.28	11—56	Unstable/quench
$H_2/O_2/N_2$	d7	0.6	11	1.00	1.40	0.12	0.56	370	690	3.79	0.95	6.6	310	0.32	63-75	Unstable/quench
$H_2/O_2/N_2$	d7	0.6	11.5	1.00	1.40	0.14	0.51	370	700	3.90	0.96	6.5	340	0.37	84-85	Choked flame
$H_2/O_2/N_2$	d7	0.6	12.7	1.00	1.40	0.18	0.40	370	730	4.17	0.98	6.2	430	0.50	79	Choked flame
$H_2/O_2/N_2$	d7	0.6	13	1.00	1.40	0.20	0.38	370	730	4.23	0.99	6.1	450	0.53	74-85	Choked flame
$H_2/O_2/N_2$	d7	0.6	15	1.00	1.40	0.30	0.28	370	770	4.66	1.03	5.7	620	0.81	83	Choked flame
$H_2/O_2/N_2$	d8	0.9	13	1.00	1.40	0.20	0.38	370	730	4.23	0.99	6.1	140	0.53	73	Choked flame
H_2/O_2/He	e1	0.09	8	1.00	1.63	0.23	1.68	890	1750	3.93	1.82	7.6	2	0.26	81-85	Unstable/slow
H_2/O_2/He	e1	0.09	12	1.00	1.60	0.77	0.58	850	1870	5.18	1.73	6.1	7	0.91	78-79	Unstable/slow
H_2/O_2/He	e1	0.09	15	1.00	1.59	1.51	0.32	820	1900	5.99	1.67	5.4	12	1.85	89-91	Unstable/slow
H_2/O_2/He	e1	0.09	17	1.00	1.58	2.20	0.23	800	1890	6.40	1.63	5.0	17	2.76	86	Detonation
H_2/O_2/He	e2	0.3	8	1.00	1.63	0.23	1.68	890	1750	3.93	1.82	7.6	100	0.26	17	Unstable/quench
H_2/O_2/He	e2	0.3	9	1.00	1.62	0.32	1.23	880	1790	4.26	1.80	7.2	140	0.37	50	Unstable/quench
H_2/O_2/He	e2	0.3	9	1.00	1.62	0.32	1.23	880	1790	4.26	1.80	7.2	140	0.37	71	Quasi-detonation
H_2/O_2/He	e2	0.3	10	1.00	1.62	0.45	0.93	870	1820	4.58	1.78	6.8	190	0.51	78-80	Quasi-detonation
H_2/O_2/He	e3	0.6	10.5	1.00	1.61	0.52	0.82	860	1840	4.73	1.76	6.6	210	0.60	81	Choked flame
H_2/O_2/He	e3	0.6	11	1.00	1.61	0.59	0.73	860	1850	4.89	1.75	6.5	240	0.69	81-82	Choked flame
H_2/O_2/He	e3	0.6	13	1.00	1.60	0.98	0.47	840	1900	5.47	1.71	5.9	370	1.17	81	Choked flame
H_2/O_2/He	e3	0.6	15	1.00	1.59	1.51	0.32	820	1900	5.99	1.67	5.4	550	1.85	84	Quasi-detonation

Table 2: (continued)

Mixture	Label	BR	$\%H_2$	ϕ	γ_r	S_L, m/s	δ_T, mm	c_{sr}, m/s	c_{sp}, m/s	σ	Le	β	L_T/δ	1000 S_L/c_{sr}	% of fuel consumed	Results
$H_2/O_2/Ar$	e5	0.09	8	1.00	1.62	0.12	0.53	330	640	3.93	0.97	7.1	7	0.35	73-78	Unstable/slow
$H_2/O_2/Ar$	e5	0.09	10	1.00	1.61	0.23	0.32	330	690	4.58	1.02	6.3	12	0.69	81-82	Unstable/slow
$H_2/O_2/Ar$	e5	0.09	13	1.00	1.60	0.50	0.18	340	760	5.47	1.10	5.4	21	1.49	79-82	Unstable/slow
$H_2/O_2/Ar$	e5	0.09	15	1.00	1.59	0.77	0.13	340	790	5.99	1.15	5.0	29	2.27	82	Detonation
$H_2/O_2/Ar$	e6	0.3	7	1.00	1.63	0.08	0.72	330	610	3.59	0.94	7.5	240	0.24	29	Unstable/quench
$H_2/O_2/Ar$	e6	0.3	8	1.00	1.62	0.12	0.53	330	640	3.93	0.97	7.1	330	0.35	65-75	Quasi-detonation
$H_2/O_2/Ar$	e6	0.3	10	1.00	1.61	0.23	0.32	330	690	4.58	1.02	6.3	550	0.69	70-72	Quasi-detonation
$H_2/O_2/Ar$	e6	0.3	12	1.00	1.60	0.39	0.21	330	740	5.18	1.07	5.7	820	1.18	74	Quasi-detonation
$H_2/O_2/Ar$	e7	0.6	8.5	1.00	1.61	0.14	0.46	330	660	4.09	0.98	6.9	380	0.43	72	Choked flame
$H_2/O_2/Ar$	e7	0.6	8.75	1.00	1.62	0.15	0.43	330	660	4.18	0.99	6.8	400	0.46	75-77	Choked flame
$H_2/O_2/Ar$	e7	0.6	9	1.00	1.62	0.17	0.40	330	670	4.26	0.99	6.7	430	0.50	79	Choked flame
$H_2/O_2/Ar$	e7	0.6	10	1.00	1.61	0.23	0.32	330	690	4.58	1.02	6.3	550	0.69	85	Choked flame
$H_2/O_2/Ar$	e7	0.6	11	1.00	1.61	0.30	0.26	330	720	4.88	1.05	6.0	680	0.91	82	Choked flame
$H_2/O_2/Ar$	e7	0.6	12	1.00	1.60	0.39	0.21	330	740	5.18	1.07	5.7	820	1.18	79-83	Quasi-detonation
$H_2/O_2/Ar$	e7	0.6	13	1.00	1.60	0.50	0.18	340	760	5.47	1.10	5.4	980	1.49	80-82	Quasi-detonation

Table 3: Mixture properties and results of 350-mm tube experiments

Mixture	Label	BR	%H_2	ϕ	γ_r	S_L, m/s	δ_T, mm	c_{sr}, m/s	c_{sp}, m/s	σ	Le	β	L_T/δ	1000 S_L/c_{sr}	Results
H_2/air	g1	0.6	9	0.24	1.40	0.17	0.38	360	640	3.31	0.34	6.9	910	0.48	Unstable/slow
H_2/air	g1	0.6	9.5	0.25	1.40	0.21	0.33	360	650	3.43	0.35	6.7	1060	0.58	Unstable/slow
H_2/air	g1	0.6	10	0.26	1.40	0.25	0.29	360	660	3.54	0.35	6.6	1210	0.68	Unstable/slow
H_2/air	g1	0.6	11	0.29	1.40	0.33	0.23	360	680	3.77	0.36	6.3	1510	0.92	Choked flame
H_2/air	g1	0.6	12	0.32	1.40	0.43	0.19	360	700	3.99	0.37	6.0	1820	1.19	Choked flame
H_2/air	g1	0.6	17.31	0.50	1.40	1.09	0.11	380	810	5.09	0.41	4.9	3260	2.89	Choked flame
H_2/air	g1	0.6	29.5	1.00	1.40	2.67	0.08	400	980	6.99	1.38	3.6	4490	6.61	Quasi-detonation
H_2/air	g1	0.6	30	1.02	1.40	2.72	0.08	400	980	7.02	1.40	3.6	4520	6.72	Quasi-detonation
H_2/air	g1	0.6	45.59	1.99	1.40	3.30	0.07	450	1070	6.23	2.45	7.4	4680	7.27	Quasi-detonation
H_2/air	g1	0.6	62.62	3.99	1.40	1.81	0.15	530	1140	4.90	3.34	9.2	2400	3.40	Choked flame
H_2/air	g1	0.6	70	5.55	1.40	0.91	0.29	580	1170	4.24	3.83	10.4	1190	1.55	Choked flame
H_2/air	g1	0.6	72	6.12	1.40	0.68	0.39	600	1170	4.05	3.97	10.8	900	1.13	Choked flame
H_2/air	g1	0.6	75	7.14	1.40	0.38	0.70	630	1190	3.76	4.20	11.4	500	0.60	Choked flame
$H_2/O_2/N_2$	g2	0.6	10	1.00	1.40	0.09	0.70	360	670	3.56	0.92	6.9	500	0.24	Unstable/quench
$H_2/O_2/N_2$	g2	0.6	10	1.00	1.40	0.09	0.70	360	670	3.56	0.92	6.9	500	0.24	Unstable/slow
$H_2/O_2/N_2$	g2	0.6	11	1.00	1.40	0.12	0.56	370	690	3.79	0.95	6.6	630	0.32	Choked flame
$H_2/O_2/N_2$	g2	0.6	12	1.00	1.40	0.15	0.46	370	710	4.01	0.97	6.4	760	0.42	Choked flame
H_2/O_2/He	g3	0.6	8.5	1.00	1.63	0.27	1.43	890	1770	4.10	1.81	7.4	240	0.31	Choked flame
H_2/O_2/He	g3	0.6	9	1.00	1.62	0.32	1.23	880	1790	4.26	1.80	7.2	280	0.37	Choked flame
H_2/O_2/He	g3	0.6	10	1.00	1.62	0.45	0.93	870	1820	4.58	1.78	6.8	380	0.51	Choked flame
H_2/O_2/He	g3	0.6	11	1.00	1.61	0.59	0.73	860	1850	4.89	1.75	6.5	480	0.69	Choked flame
H_2/O_2/He	g3	0.6	11.68	1.00	1.61	0.71	0.62	850	1870	5.09	1.74	6.2	570	0.84	Choked flame
H_2/O_2/He	g3	0.6	12	1.00	1.60	0.77	0.58	850	1870	5.18	1.73	6.1	610	0.91	Choked flame
H_2/O_2/He	g3	0.6	13.5	1.00	1.60	1.10	0.42	830	1900	5.61	1.70	5.7	830	1.32	Quasi-detonation
H_2/O_2/Ar	g4	0.6	8	1.00	1.62	0.12	0.53	330	640	3.93	0.97	7.1	660	0.35	Quasi-detonation
H_2/O_2/Ar	g4	0.6	9	1.00	1.62	0.17	0.40	330	670	4.26	0.99	6.7	870	0.50	Quasi-detonation

Table 3: (continued)

Mixture	Label	BR	%H_2	ϕ	γ_r	S_L, m/s	δ_T, mm	c_{sr}, m/s	c_{sp}, m/s	σ	Le	β	L_T/δ	1000 S_L/c_{sr}	Results
$H_2/O_2/CO_2$	g5	0.6	16	1.00	1.30	0.11	0.41	300	540	3.72	0.87	7.2	840	0.38	Unstable/quench
$H_2/O_2/CO_2$	g5	0.6	17	1.00	1.30	0.14	0.36	300	560	3.87	0.90	7.0	970	0.47	Unstable/slow
$H_2/O_2/CO_2$	g5	0.6	18	1.00	1.30	0.17	0.32	300	570	4.02	0.93	6.8	1100	0.56	Choked flame
$H_2/O_2/CO_2$	g5	0.6	20	1.00	1.31	0.24	0.26	300	600	4.32	0.99	6.4	1360	0.77	Choked flame
$H_2/O_2/CO_2$	g5	0.6	30	1.00	1.32	0.75	0.14	330	730	5.70	1.34	4.9	2490	2.26	Choked flame
H_2/air/CO_2	g6	0.6	10.39	0.50	1.34	0.12	0.35	320	550	3.18	0.26	6.9	1000	0.38	Unstable/slow
H_2/air/CO_2	g6	0.6	11.26	0.50	1.35	0.16	0.28	320	570	3.39	0.27	6.6	1260	0.51	Unstable/slow
H_2/air/CO_2	g6	0.6	12.12	0.50	1.35	0.22	0.22	330	600	3.60	0.27	6.3	1560	0.65	Unstable/slow
H_2/air/CO_2	g6	0.6	12.56	0.50	1.36	0.25	0.20	330	620	3.71	0.28	6.2	1720	0.74	Unstable/slow
H_2/air/CO_2	g6	0.6	12.99	0.50	1.36	0.28	0.19	340	630	3.82	0.28	6.1	1890	0.83	Choked flame
H_2/air/CO_2	g6	0.6	13.86	0.50	1.37	0.35	0.16	340	660	4.06	0.28	5.8	2250	1.03	Choked flame
H_2/air/CO_2	g6	0.6	14.72	0.50	1.37	0.44	0.13	350	700	4.30	0.29	5.6	2620	1.26	Choked flame
H_2/air/CO_2	g6	0.6	15.59	0.50	1.38	0.54	0.12	360	730	4.55	0.30	5.3	3020	1.51	Choked flame
H_2/air/CO_2	g6	0.6	16.45	0.50	1.39	0.65	0.10	370	770	4.82	0.30	5.1	3420	1.79	Choked flame
H_2/air/CO_2	g6	0.6	16.89	0.50	1.39	0.72	0.10	370	790	4.96	0.31	5.0	3630	1.93	Choked flame
H_2/air/CO_2	g6	0.6	14.8	0.70	1.35	0.35	0.16	330	630	4.01	0.29	5.8	2170	1.08	Unstable/slow
H_2/air/CO_2	g7	0.6	15.2	1.00	1.33	0.33	0.17	320	600	3.91	0.78	5.9	2010	1.04	Choked flame
H_2/air/CO_2	g7	0.6	15.6	0.99	1.33	0.36	0.16	320	610	3.99	0.79	5.8	2130	1.13	Choked flame
H_2/air/CO_2	g7	0.6	16.8	0.99	1.34	0.46	0.14	320	640	4.23	0.81	5.6	2510	1.40	Choked flame
H_2/air/CO_2	g7	0.6	17.7	1.00	1.34	0.54	0.13	330	660	4.42	0.83	5.4	2790	1.63	Choked flame
H_2/air/CO_2	g7	0.6	19.19	1.00	1.35	0.69	0.11	340	690	4.73	0.86	5.1	3270	2.05	Choked flame
H_2/air/CO_2	g7	0.6	20	0.95	1.35	0.80	0.10	340	720	4.95	0.88	4.9	3590	2.33	Choked flame
H_2/air/CO_2	g7	0.6	23.6	1.00	1.37	1.24	0.08	360	810	5.69	0.96	4.3	4570	3.44	Choked flame
H_2/air/CO_2	g7	0.6	25	0.99	1.37	1.45	0.07	370	850	6.00	0.99	4.1	4920	3.91	Choked flame
H_2/air/CO_2	g7	0.6	26	1.01	1.38	1.57	0.07	380	870	6.18	1.02	4.0	5090	4.18	Choked flame
H_2/air/CO_2	g7	0.6	26.5	0.99	1.38	1.67	0.07	380	890	6.32	1.03	3.9	5240	4.38	Quasi-detonation
H_2/air/CO_2	g7	0.6	28	0.99	1.39	1.90	0.06	390	930	6.64	1.07	3.7	5530	4.84	Quasi-detonation

Table 3: (continued)

Mixture	Label	BR	%H_2	ϕ	γ_r	S_L, m/s	δ_T, mm	c_{sr}, m/s	c_{sp}, m/s	σ	Le	β	L_T/δ	1000 S_L/c_{sr}	Results
H_2/air/CO_2	g8	0.6	26.21	1.99	1.34	0.07	1.02	340	600	3.45	1.84	11.9	340	0.20	Unstable/quench
H_2/air/CO_2	g8	0.6	27.35	1.99	1.34	0.09	0.80	340	620	3.57	1.89	11.7	440	0.26	Unstable/slow
H_2/air/CO_2	g8	0.6	28.49	1.99	1.34	0.12	0.63	350	640	3.69	1.94	11.4	560	0.35	Choked flame
H_2/air/CO_2	g8	0.6	29.63	1.99	1.35	0.16	0.50	350	660	3.82	1.45	11.1	700	0.45	Choked flame
H_2/air/CO_2	g8	0.6	31.91	1.99	1.35	0.27	0.33	360	700	4.09	1.53	10.5	1060	0.74	Choked flame
H_2/air/CO_2	g8	0.6	36.5	2.00	1.37	0.69	0.16	390	800	4.68	1.70	9.5	2200	1.77	Choked flame
H_2/air/CO_2	g8	0.6	41	1.99	1.38	1.59	0.08	420	920	5.39	1.88	8.4	4140	3.82	Choked flame
H_2/air/CO_2	g8	0.6	43.31	1.99	1.39	2.33	0.06	430	990	5.80	1.98	7.9	5450	5.36	Choked flame
H_2/air/CO_2	g8	0.6	43.88	1.99	1.39	2.55	0.06	440	1010	5.90	2.00	7.7	5820	5.80	Quasi-detonation
H_2/air/CO_2	g8	0.6	44.45	1.99	1.40	2.78	0.06	440	1030	6.01	2.03	7.6	6200	6.27	Quasi-detonation
H_2/air/CO_2	g9	0.6	47.75	3.99	1.36	0.10	1.08	410	720	3.36	2.16	12.2	320	0.24	Unstable/slow
H_2/air/CO_2	g9	0.6	48.5	3.98	1.36	0.12	0.95	420	730	3.42	2.20	12.0	370	0.28	Unstable/slow
H_2/air/CO_2	g9	0.6	50	3.97	1.37	0.16	0.73	420	770	3.55	2.27	11.7	480	0.38	Choked flame
H_2/air/CO_2	g9	0.6	53.2	3.98	1.38	0.29	0.45	450	840	3.82	2.43	11.2	770	0.66	Choked flame
H_2/air/CO_2	g9	0.6	56	3.92	1.38	0.56	0.27	470	920	4.17	2.58	10.5	1310	1.20	Choked flame
H_2/air/CO_2	g9	0.6	59.5	3.99	1.39	0.94	0.18	500	1020	4.50	2.78	9.9	1940	1.89	Choked flame

Table 4: Mixture properties and results of 520-mm tube experiments

Mixture	Label	BR	%H_2	ϕ	γ_r	S_L, m/s	δ_T, mm	c_{sr}, m/s	c_{sp}, m/s	σ	Le	β	L_T/δ	1000 S_L/c_{sr}	% of fuel consumed	Results
H_2/air	t1	0.6	9	0.24	1.40	0.17	0.38	360	640	3.31	0.34	6.9	1350	0.48	35-68	Unstable/slow
H_2/air	t1	0.6	9.5	0.25	1.40	0.21	0.33	360	650	3.43	0.35	6.7	1570	0.58	70	Unstable/slow
H_2/air	t1	0.6	10	0.26	1.40	0.25	0.29	360	660	3.54	0.35	6.6	1790	0.68	76-88	Unstable/slow
H_2/air	t1	0.6	10.9	0.29	1.40	0.33	0.23	360	680	3.77	0.36	6.3	2250	0.92	93	Choked flame
H_2/O_2/He	t2	0.6	11	1.00	1.61	0.59	0.73	860	1850	4.89	1.75	6.5	720	0.69	88	Choked flame
H_2/O_2/He	t2	0.6	11.5	1.00	1.61	0.68	0.64	850	1860	5.04	1.74	6.3	810	0.80	88	Choked flame
H_2/O_2/He	t2	0.6	11.5	1.00	1.61	0.68	0.64	850	1860	5.04	1.74	6.3	810	0.80	84	Quasi-detonation
H_2/air	t3	0.3	8	0.21	1.40	0.11	0.54	360	610	3.08	0.34	7.2	950	0.31	74	Unstable/slow
H_2/air	t3	0.3	9	0.24	1.40	0.17	0.38	360	640	3.31	0.34	6.9	1350	0.48	72-74	Unstable/slow
H_2/air	t3	0.3	10	0.26	1.40	0.25	0.29	360	660	3.54	0.35	6.6	1790	0.68	67-73	Unstable/slow
H_2/air	t3	0.3	11	0.29	1.40	0.33	0.23	360	680	3.77	0.36	6.3	2250	0.92	76	Unstable/slow
H_2/air	t3	0.3	11	0.29	1.40	0.33	0.23	360	680	3.77	0.36	6.3	2250	0.92	85-87	Choked flame
H_2/air	t3	0.3	12	0.32	1.40	0.43	0.19	360	700	3.99	0.37	6.0	2710	1.19	90	Choked flame
H_2/air	t3	0.3	13	0.36	1.40	0.54	0.16	370	720	4.21	0.38	5.8	3160	1.47	91	Choked flame
H_2/air	t4	0.09	8	0.21	1.40	0.11	0.54	360	610	3.08	0.34	7.2	21	0.31	5	Unstable/slow
H_2/air	t4	0.09	9	0.24	1.40	0.17	0.38	360	640	3.31	0.34	6.9	30	0.48	56	Unstable/slow
H_2/air	t4	0.09	10	0.26	1.40	0.25	0.29	360	660	3.54	0.35	6.6	39	0.68	87	Unstable/slow
H_2/air	t4	0.09	14	0.39	1.40	0.66	0.14	370	740	4.42	0.39	5.6	79	1.78	93	Unstable/slow
H_2/air	t4	0.09	16	0.45	1.40	0.91	0.12	370	780	4.83	0.40	5.2	96	2.44	91	Unstable/slow
H_2/air	t4	0.09	18	0.52	1.40	1.18	0.10	380	820	5.23	0.42	4.8	110	3.13	94	Detonation